risk of QTc prolongation for an individual antipsychotic in a dose-dependent manner, particularly for second-generation antipsychotics (SGAs). Some case reports have indicated that SGAs can induce QTc prolongation (Dineen et al., 2003; Vieweg, 2003). However, such anecdotal reports do not provide clear evidence of whether SGAs increase the risk of QTc prolongation, as in first-generation antipsychotics (FGAs), in a real-world setting. This study examined the risk of QTc prolongation of antipsychotic drugs in a large clinical sample from Japan. Japan is known to use higher doses of antipsychotics (Bitter et al., 2003), providing a unique opportunity to investigate the risk of QTc prolongation in a wide range of antipsychotic doses.

2. Methods

2.1. Patients

Clinical information, including data on QTc intervals, was collected from inpatients with schizophrenia who were diagnosed according to the Diagnostic and Statistical Manual of Mental Disorders, 4th ed. (DSM-IV) in four independent hospitals. Approval from the ethics committee of each hospital was obtained. Data collection on all inpatients with schizophrenia was begun on the following dates in three psychiatric hospitals Biwako Hospital, Toyosato Hospital, and Minakuchi Hospital: February 2, 2007; February 3, 2007; and July 29, 2007, respectively. In the fourth hospital, the National Center of Neurology and Psychiatry Hospital, clinical records were collected for all patients who were admitted to its psychiatric wards between 1998 and 2007. A total of 1065 inpatients were included from the four hospitals, and all of them underwent ECG screening. Among them, 37 patients were excluded due to hypokalemia (serum potassium <3.5 mEq/L), which can induce QTc interval prolongation (Elming et al., 2003; Taylor, 2003). Two were excluded because of hypothyroidism, and nine because of cardiac disease (four patients with right bundle branch block, two with post-acute myocardial infarction, one with WPW syndrome, one with atrial–ventricular block, and one who underwent surgery for atrial septal defect). The remaining 1017 patients had a mean age of 42.6 years (S.D., 18.2) and were included in the analysis.

2.2. Procedure

A standard 12-lead ECG was recorded at 25 mm/s. Because the QTc interval is influenced by heart rate, it was corrected by Bazett's formula (QTc: $QTc = QT/RR^{1/2}$) (Bazett, 1920). An ECG recording showing the longest QTc interval was selected for each patient whose ECG was recorded two or more times. The QTc was measured automatically by a program on the ECG apparatus (MAC 5500 with 12SL algorithm by GE health care [Amersham Place, Little Chalfont, Buckinghamshire, UK]). For patients with a QTc > 430 ms, QTc and RR intervals were measured manually for the chest lead with the maximal T-wave amplitude, according to Charbit et al. (2006). The end of the T-wave was determined as the intersection between the tangent to the steepest downslope of the T-wave and the isoelectric line. QTc prolongation was defined as a QTc length of more than 470 ms in males and more than 480 ms in females, as 99% of "healthy" people can be excluded by this cut-off value (Taggart et al., 2007). One of the coauthors (M.H.), a cardiologist who specializes in arrhythmias, trained the authors on how to evaluate an ECG recording. Information on drugs administered within 24 h of the ECG recording was obtained. Table 1 shows the distribution of drugs that were administered in more than 3% of the patients and the prevalence of QTc prolongation for each medication. One hundred forty-two patients were drug free when the ECG was recorded, because they were given the test at admission before they had taken any drugs. Two hundred sixty-five patients were on monotherapy. Doses of antipsychotics, antiparkinsonian drugs, and benzodiazepines were converted into those of CP, biperiden, and diazepam equivalents, respectively (Inagaki and Inada, 2006). Subjects who were coadministered medical drugs (i.e., non psychotropic drugs) with an increased risk of producing torsade de pointes were excluded (Chan et al., 2007).

Table 1
Medication and rate of QTc prolongation in 1017 patients. Drugs which were administrated to more than 3% of patients are shown.

Administrated drugs	No. of Patients $n = 1017$ (100%)	Mean dose (SD), mg	No. of patients (%) with QTc prolongation (male: >470 ms, female > 480 ms)
Equivalent dose			
CP eq.	875 (86)	963.0 (879.0)	23 (2.6)
Diazepam eq.	672 (66)	14.6 (14.6)	18 (2.7)
Biperiden eq.	645 (63)	3.8 (2.2)	19 (2.9)
Mood stabilizer			
CBZ	74 (7)	478.9 (201.8)	3 (4.1)
VPA	54 (5)	650.0 (334.1)	1 (1.9)
Lithium	47 (5)	587.2 (199.6)	4 (8.5)
Antipsychotics			
HPD	375 (37)	15.9 (12.6)	16 (4.3)
CP	299 (29)	190.5 (198.7)	9 (3.0)
LP	258 (25)	91.9 (94.5)	14 (5.4)
Risperidone	248 (24)	5.6 (3.7)	4 (1.6)
Zotepine	116 (11)	179.9 (124.9)	3 (2.6)
Olanzapine	104 (10)	15.6 (6.4)	0 (0.0)
Quetiapine	60 (6)	375.5 (258.5)	0 (0.0)
Bromperidol	49 (5)	10.7 (8.6)	0 (0.0)
Sultopride	49 (5)	1032.9 (810.2)	10 (20.4)
HPD iv	47 (5)	16.0 (10.5)	8 (17.0)

Abbreviations: eq = equivalent; HPD = haloperidol, CP = chlorpromazine; LP = levomepromazine, CBZ = carbamazepine, VPA = sodium valproate; No. = Number, SD = standard deviation.

2.3. Statistical analyses

First, logistic regression analysis was applied to examine risk factors for QTc prolongation. Age, sex, antipsychotic dose (CP equivalent), benzodiazepine dose (diazepam equivalent), and antiparkinsonian drug dose (biperiden equivalent) were included in the backward stepwise regression model. In the second analysis, age, sex, and individual antipsychotic doses were entered as independent variables in the logistic regression analysis. Then, the adjusted relative risks of important explanatory variables were calculated via the backward stepwise regression analysis. Drugs that were administrated in more than 3% of the patients were analyzed.

Linear regression analysis was used to determine which antipsychotics lengthened the QTc interval in a dose-dependent manner, as the antipsychotic dose was entered as a continuous variable. Then, the adjusted coefficients were calculated using the stepwise selection model. Age, sex, and individual antipsychotic doses were entered as independent variables.

The χ^2 test was used to examine the risk-increasing effect of excessive use of antipsychotics (cut-off points of 1000 or 1500 mg/day of CP equivalent). All statistical analyses were performed using the SPSS, version 13.0 (SPSS Japan, Inc., Tokyo, Japan). All p-values reported are two tailed. Statistical significance was considered when p-value was less than 0.05.

3. Results

The prevalence of QTc prolongation (>470 ms in male and >480 ms in female) was 2.5% (male: 3.7%; female: 1.0%). Logistic regression analysis showed that the antipsychotic dose was a significant risk factor for QTc prolongation (Table 2), whereas antiparkinsonian drugs, benzodiazepines, and mood stabilizers were not risk factors for QTc prolongation. Administration of antipsychotic doses greater than 1000 and 1500 mg/day of CP equivalent was found

Table 2
Result of logistic regression analysis on the risk of QTc prolongation for standardized doses.

	Unadjusted relative risk (95% CI)	Adjusted relative risk (95% CI)
Age	0.97 (0.94–0.99)	
Sex (risk of female)	0.33 (0.12–0.95)	
CP eq. (100 mg)	1.08 (1.05–1.12)*	1.07 (1.04–1.10)*
Diazepam eq. (1 mg)	1.01 (0.98–1.04)	
Biperiden eq. (1 mg)	0.87 (0.72–1.06)	
CBZ (100 mg)	1.00 (1.00–1.00)	
VPA (100 mg)	1.00 (0.99–1.00)	
Lithium (100 mg)	1.00 (1.00–1.01)	
	The Hosmer–Lemeshow Goodness-of-Fit Test $x^2 = 4.77$ $df = 8$ $p = 0.85$	The Hosmer–Lemeshow Goodness-of-Fit Test $x^2 = 5.15$ $df = 8$ $p = 0.74$

*$p < 0.001$.
Abbreviations: eq = equivalent, CP = chlorpromazine, CBZ = carbamazepine; VPA = sodium valproate, CI = confidence interval.

to increase the risk of QTc prolongation 1.97 fold (95% CI, 1.48–2.59, $p < 0.001$) and 2.76 fold (95% CI, 1.80–4.18, $p < 0.001$), respectively, when compared to their counterparts. On examination of individual antipsychotics, haloperidol intravenous injection (HPDiv), CP, and sultopride were found to increase the risk of QTc prolongation (Table 3).

In the stepwise selection model of the multiple linear regression analysis, CP, HPDiv, levomepromazine (LP), and sultopride were found to lengthen the QTc interval. Age was also indicated as a risk factor for QTc lengthening. Adjusted coefficients for CP, HPDiv, LP, sultopride, and sex are shown in Table 4. Adding 100 mg of LP, for example, extended the QTc interval by 4.65 ms. Bromperidol, olanzapine, quetiapine, risperidone, and zotepine had no significant lengthening effect on the QTc interval.

Table 3
Result of logistic regression analysis on the risk of QTc prolongation for each antipsychotic drug.

	Unadjusted relative risk (95%CI)	Adjusted relative risk (95%CI)
Age	0.99 (0.96–1.03)	
Sex (risk of female)	0.38 (1.26–1.16)	
HPD (2 mg)	0.99 (0.92–1.06)	
CP (100 mg)	1.37 (1.13–1.67)*	1.37 (1.14–1.64)*
LP (100 mg)	1.55 (0.92–2.61)	
Risperidone (1 mg)	1.01 (0.84–1.12)	
Zotepine (66 mg)	0.91 (0.62–1.34)	
Olanzapine (2.5 mg)	0.00 (0.00 to >100)	
Quetiapine (66 mg)	0.00 (0.00 to >100)	
Bromperidol (2 mg)	0.00 (0.00 to >100)	
Sultopride (200 mg)	1.40 (1.23–1.60)**	1.45 (1.28–1.63)**
HPD iv (2 mg)	1.26 (1.13–1.40)**	1.29 (1.18–1.43)**
	The Hosmer–Lemeshow Goodness-of-Fit Test $x^2 = 5.04$ $df = 8$ $p = 0.75$	The Hosmer–Lemeshow Goodness-of-Fit Test $x^2 = 17.81$ $df = 8$ $p = 0.013$

*$p < 0.005$.
**$p < 0.001$.
Abbreviations: HPD = haloperidol, CP = chlorpromazine, LP = levomepromazine, iv = intravenous injection, CI = confidence interval.

4. Discussion

In a large clinical sample, we confirmed that a daily dose of antipsychotics (CP equivalents) was associated with a dose-dependent increased risk of QTc prolongation; however, the use of antiparkinsonian drugs, benzodiazepines, and mood stabilizers did not significantly increase this risk. With regard to individual antipsychotics, CP, HPDiv, and sultopride were shown to significantly increase the risk of QTc prolongation. CP, HPDiv, LP, and sultopride were found to significantly lengthen the QTc interval, whereas HPD, bromperidol, olanzapine, quetiapine, risperidone, and zotepine were not.

Our observation that a daily dose of antipsychotics was associated with a risk of QTc prolongation is consistent with previous studies (Reilly et al., 2000; Warner et al., 1996). In our sample, antipsychotic doses of more than 1000 and 1500 mg/day of CP equivalents were found to increase the risk of QTc prolongation by approximately 2.0 and 3.0 fold, respectively, when compared to their counterparts. Reilly et al. also reported that a high dose (1000 to 2000 mg/day) and a very high dose (>2000 mg/day) predicted QTc prolongation [odds ratio (OR), 5.3 and 8.2, respectively] (Reilly et al., 2000). Warner et al. reported an OR of 4.3 for doses higher than 2000 mg/day (Warner et al., 1996). In contrast to antipsychotics, mood stabilizers showed no significant risk-increasing effect. This is consistent with a previous finding, which showed that lithium or carbamazepine did not significantly increase the risk of QTc prolongation (Reilly et al., 2000). However, a recent study suggested that lithium increases the QTc interval significantly (18.6 ms; 95% CI, 4.8–32.4 ms) (van Noord et al., 2009). Furthermore, lithium is known to cause T-wave changes (Mitchell and Mackenzie, 1982; Reilly et al., 2000) that may lead to torsade de pointes when combined with a QTc-lengthening antipsychotic (Liberatore and Robinson, 1984). Thus, the use of lithium requires careful ECG monitoring. With respect to valproate, our study may be the first to investigate the risk of QTc prolongation for this drug in a clinical setting. With regard to coadministered benzodiazepine and antiparkinsonian drugs, our results suggest no significant effect on QTc prolongation. Although some patients taking diazepam and biperiden equivalent showed QTc interval prolongation (Table 1), the results of logistic regression analysis showed no significant risk-increasing effect of these drugs (Table 2). Therefore, these patients were also taking chlorpromazine equivalent and it was the chlorpromazine equivalent that explained the QTc interval prolongation. Indeed, to our knowledge, there has been no study reporting that these drugs cause QTc prolongation or torsade de pointes.

With respect to individual antipsychotics, previous studies have reported that thioridazine, intravenous droperidol, sertindole, and ziprasidone are associated with a strong risk-increasing effect on QTc prolongation (Czekalla et al., 2001a; Harrigan et al., 2004; Taylor,

Table 4
QTc prolongation effect of each antipsychotic by linear regression model.

	Forced entry model	Stepwise selection model
	Coefficient (95% CI)	Coefficient (95% CI)
Age	0.19 (0.10–0.28)*	0.20 (0.11–0.29)*
Sex (risk of female)	3.22 (−0.01–6.44)	
HPD (2 mg)	0.42 (0.09–0.76)	
CP (100 mg)	3.91 (2.69–5.13)*	3.82 (2.62–5.02)*
LP (100 mg)	4.87 (2.14–7.60)*	4.65 (1.94–7.37)*
Risperidone (1 mg)	0.07 (−0.47–0.61)	
Zotepine (66 mg)	−0.36 (−1.91–1.20)	
Olanzapine (2.5 mg)	0.30 (−0.47–1.08)	
Quetiapine (66 mg)	0.11 (−0.87–1.09)	
Bromperidol (2 mg)	0.08 (−1.00–1.16)	
Sultopride (200 mg)	3.65 (2.48–4.82)*	3.56 (2.41–4.72)*
HPD iv (2 mg)	3.16 (2.36–3.96)*	3.13 (2.34–3.93)*

*$p < 0.001$.
Abbreviations: HPD = haloperidol, CP = chlorpromazine, LP = levomepromazine; iv = intravenous injection, CI = confidence interval.

2003). In Japan, commercial use of thioridazine ended in 2005; intravenous droperidol has not been used in psychiatric treatment; and sertindole and ziprasidone have not been introduced. Thus, we could not confirm the effect of these drugs. However, our results provide robust evidence that HPDiv increases the risk of QTc prolongation. This concurs with Hatta et al. who compared the differences in QTc length among psychiatric emergency patients who received intravenous flunitrazepam alone and those who received intravenous flunitrazepam and haloperidol and found that the latter group showed significantly longer QTc intervals than the former (Hatta et al., 2001). Vieweg et al. (2009) reviewed the literature and identified cases of patients aged ≥60 years who developed QTc interval prolongation, polymorphic ventricular tachycardia/torsade de pointes and/or sudden cardiac death while taking antipsychotic or antidepressant drugs or a combination of these medications. Among such cases, most frequently reported medication was HPDiv (14 out of 37 cases). These findings and ours support the recent alert of the U.S. Food and Drug Administration warning that HPDiv increases the risk of QTc prolongation and torsade de pointes based on at least 28 cases reported in the literature (U.S. Food and Drug Administration Cfdear, 2007). Oral HPD, in contrast, was found to have no statistically significant risk-increasing effect on QTc prolongation, although it had a significant QTc-lengthening effect. Previous findings have suggested that oral HPD at low or moderate doses had no clear effect on QTc, but that it is associated with QTc prolongation and torsade de pointes at higher clinical doses (>20 mg/day) (Czekalla et al., 2001a; Taylor, 2003). Taken together, excessively high blood levels of the drug after an intravenous injection or oral intake of high doses may be critical for the effect of HPD. Regarding bromperidol (oral use only), a chemically similar butyrophenone to HPD, we obtained no evidence for its effect on QTc prolongation or lengthening. To our knowledge, this is the first study to examine bromperidol for such effects. Further studies are warranted to confirm our results. With respect to CP, we detected significant effects on both QTc prolongation and QTc lengthening, which is consistent with previous findings, suggesting an intermediate effect of CP on QTc (i.e., a weaker effect than that of thioridazine, but stronger than oral HPD) (Czekalla et al., 2001a; Mehtonen et al., 1991; Witchel et al., 2003), although there have been some reports of no significant risk-increasing effect of CP (Reilly et al., 2000; Strachan et al., 2004). LP, another phenothiazine, was also found to lengthen the QTc interval in the multiple regression analysis. In the logistic regression, statistical significance was nearly achieved ($p=0.06$, Table 3). These results suggest that LP is likely to increase the risk of QTc prolongation. Although there have been little data on LP in relation to QTc in the literature, an association between sudden death and the use of phenothiazines is prominent, and LP might have been involved in such deaths (Mehtonen et al., 1991). Finally, sultopride, a benzamide derivative, was found to significantly increase the risk of QTc prolongation and QTc lengthening. To our knowledge, this is the first time that such evidence has been obtained for sultopride. Further studies are warranted to confirm our results.

Our results provide no evidence for the possible risk-increasing effect of the examined SGAs (olanzapine, quetiapine, risperidone, and zotepine) on QTc prolongation. Recently, Ray et al. (2009) reported that atypical antipsychotics double the risk of sudden cardiac death when compared with nonusers of antipsychotic drugs, a finding that contradicts our data. However, SGAs can induce weight gain, insulin resistance, and dyslipidemia (Tschoner et al., 2009), all of which are risk factors for ischemic heart diseases. Therefore, the increased sudden death observed by Ray et al. (2009) could be attributable to the increased risk of ischemic heart diseases rather than torsade de pointes due to QTc prolongation. The Pfizer 054 study (2000) reported that SGAs, such as risperidone, quetiapine, ziprasidone, and olanzapine, induced QTc interval prolongation. In the review of Czekalla et al. (2001a), it was suggested that risperidone and quetiapine could lengthen the QTc interval, although the effect observed was smaller than that of thioridazine and chlorpromazine. Olanzapine, in particular, was reported to have little effect on the QTc-interval length (Czekalla et al., 2001b). Dineen et al. (2003) reported the case of a patient who was treated with olanzapine and showed an abnormal QTc interval. Vieweg (2003) reviewed the literature and found nine cases in which QTc prolongation was associated with SGA administration (four cases of risperidone [one case was his original case], three cases of quetiapine, and two cases of ziprasidone). Taken together, although our results suggest that the SGAs (olanzapine, quetiapine, risperidone, and zotepine) are less likely to produce QTc interval prolongation than the FGAs examined herein, the SGAs can also cause QTc prolongation. Thus, further investigations with a more refined methodology are warranted. In particular, the current group-derived formula for correcting QT interval measurements to a heart rate of 60 beats per/min (QTc) are unsatisfactory (Malik, 2001), and, as pointed out by Vieweg (2003), determining the effect of drug-induced change amid the noise of random variation (regression to the mean) will require a new technology.

Female gender is known to be a risk factor for QTc prolongation (Taylor, 2003; Vieweg et al., 2009). However, we failed to detect female gender as a significant risk factor in our sample. Moreover, QTc prolongation was found more commonly in male patients than in female patients. One reason for these results was that the antipsychotic dose was substantially lower in female patients than in male patients (mean CP equivalent dose: 841 vs. 1066 mg/day; frequency of >1500 mg/day: 13.9% vs. 20.8%). In addition, because some previous studies in psychotic patients did not detect the gender difference (Chong et al., 2003; Hatta et al., 2000), such populations may have other factors that attenuate the gender difference.

There are several limitations to the study. First, we did not include medications other than psychotropic drugs in the analysis; however, the subjects included in the analysis were not coadministered other medical drugs that increased the risk for torsade de pointes (Chan et al., 2007). We also excluded patients suffering from cardiac diseases. Furthermore, psychotropic drugs that were administrated to 3% or fewer of the patients in the sample were not included in the analysis. The fact that nearly all patients received multiple drugs and a substantial proportion of participants (69%) were treated with antipsychotic polypharmacy may have made it difficult to obtain a clear result for each drug. However, there is great value in assessing the increased risk of QTc prolongation in such a practical setting. Our participants were all inpatients, and therefore individuals with severe symptomatology and those patients on high doses of antipsychotics were likely to be overrepresented. A recent study reported the possibility that an acute psychotic state itself may be a risk factor for QTc prolongation (Bar et al., 2007). Severe symptomatology might have biased the results toward an increased prevalence of the QTc interval in our subjects.

To screen QTc interval, we used an automated program, which may be fraught with errors. However, Charbit et al. (2006), for example, reported that patients with automatic QTc of <430 ms were at very low risk of having a prolonged QT interval where their definition of prolonged QTc interval was >450 ms in women and >440 ms in men. We measured QTc interval manually for patients with an automated QTc of >430 ms, although our definition of QTc prolongation was >480 ms in women and >470 ms in men. Thus, it was unlikely that we missed patients with QTc prolongation in our study. Furthermore, the reliability of the measurement algorithm of the ECG equipment (MAC 5500 with 12SL algorithm by GE health care [Amersham Place, Little Chalfont, Buckinghamshire, UK]) that we used was reported to be high. The data obtained by this algorithm was within 10 ms of the manual measurement in 95.9% of ECGs and within 15 ms in 99.3% of ECGs (Hnatkova et al., 2006). Thus, the possible effect of the use of the automated program is likely minimal. Another limitation might be that we used the chest lead with the maximal T-wave amplitude because clear T-wave leads are needed for precise

manual measurement. However, Bazett generally used limb lead II to determine his formula.

Despite these limitations, we obtained robust evidence among a large clinical sample in a real-world setting that suggested that a daily dose of antipsychotics is associated with a dose-dependent increased risk of QTc prolongation, whereas that of antiparkinsonian drugs, benzodiazepines, and mood stabilizers is not. With regard to individual antipsychotics, our results suggest that FGAs, such as HPDiv, CP, LP, and sultopride, have a risk-increasing effect on QTc prolongation and that SGAs, such as olanzapine, quetiapine, risperidone, and zotepine, are less likely to produce QTc prolongation than the FGAs. Such information may aid in clinical decision making concerning the choice of antipsychotic medication, particularly in patients who have an increased risk for arrhythmias.

5. Conclusions

We confirmed the statistical effect of chlorpromazine, levomepromazine, and HPDiv on QTc prolongation in a sample of 1017 patients with schizophrenia. Furthermore, statistical evidence for sultopride was obtained for the first time. Furthermore, in the range of the antipsychotic drugs that we examined, the data suggest that SGAs are less likely to produce QTc prolongation than FGAs, which may be useful in guiding the choice of antipsychotic drugs.

Acknowledgements

This study was supported by the Health and Labor Sciences Research Grants in Japan, Tokyo, Japan and the Dokkyo Medical University, Investigator-Initiated Research Grant (no. 2007-01-2), Mibu, Japan.

References

Bar KJ, Koschke M, Boettger MK, Berger S, Kabisch A, Sauer H, et al. Acute psychosis leads to increased QT variability in patients suffering from schizophrenia. Schizophr Res 2007;95:115–23.
Bazett HC. An analysis of the time relations of electrocardiograms. Heart 1920;7:353–70.
Bitter I, Chou JC, Ungvari GS, Tang WK, Xiang Z, Iwanami A, et al. Prescribing for inpatients with schizophrenia: an international multi-center comparative study. Pharmacopsychiatry 2003;36:143–9.
Chan A, Isbister GK, Kirkpatrick CM, Dufful SB. Drug-induced QT prolongation and torsades de pointes: evaluation of a QT nomogram. QJM 2007;100:609–15.
Charbit B, Samain E, Merckx P, Funck-Brentano C. QT interval measurement: evaluation of automatic QTc measurement and new simple method to calculate and interpret corrected QT interval. Anesthesiology 2006;104:255–60.
Chong SA, Mythily Lum A, Goh HY, Chan YH. Prolonged QTc intervals in medicated patients with schizophrenia. Hum Psychopharmacol 2003;18:647–9.
Czekalla J, Kollack-Walker S, Beasley Jr CM. Cardiac safety parameters of olanzapine: comparison with other atypical and typical antipsychotics. J Clin Psychiatry 2001a;62(Suppl 2):35–40.
Czekalla J, Beasley Jr CM, Dellva MA, Berg PH, Grundy S. Analysis of the QTc interval during olanzapine treatment of patients with schizophrenia and related psychosis. J Clin Psychiatry 2001b;62:191–8.
Dineen S, Withrow K, Voronovitch L, Munshi F, Nawbary MW, Lippmann S. QTc prolongation and high-dose olanzapine. Psychosomatics 2003;44:174–5.
Elming H, Sonne J, Lublin HK. The importance of the QT interval: a review of the literature. Acta Psychiatr Scand 2003;107:96–101.
Faber TS, Zehender M, Just H. Drug-induced torsade de pointes. Incidence, management and prevention. Drug Saf 1994;11:463–76.
Harrigan EP, Miceli JJ, Anziano R, Watsky E, Reeves KR, Cutler NR, et al. A randomized evaluation of the effects of six antipsychotic agents on QTc, in the absence and presence of metabolic inhibition. J Clin Psychopharmacol 2004;24:62–9.
Hatta K, Takahashi T, Nakamura H, Yamashiro H, Yonezawa Y. Prolonged QT interval in acute psychotic patients. Psychiatry Res 2000;94:279–85.
Hatta K, Takahashi T, Nakamura H, Yamashiro H, Asukai N, Matsuzaki I, et al. The association between intravenous haloperidol and prolonged QT interval. J Clin Psychopharmacol 2001;21:257–61.
Hennessy S, Bilker WB, Knauss JS, Margolis DJ, Kimmel SE, Reynolds RF, et al. Cardiac arrest and ventricular arrhythmia in patients taking antipsychotic drugs: cohort study using administrative data. Bmj 2002;325:1070.
Hnatkova K, Gang Y, Batchvarov VN, Malik M. Precision of QT interval measurement by advanced electrocardiographic equipment. Pacing Clin Electrophysiol 2006;29:1277–84.
Inagaki A, Inada I. Dose equivalence of psychotropic drugs: 2006-version. Jpn J Clin Psychopharmacol 2006;9:1443–7.
Liberatore MA, Robinson DS. Torsade de pointes: a mechanism for sudden death associated with neuroleptic drug therapy? J Clin Psychopharmacol 1984;4:143–6.
Malik M. Problems of heart rate correction in assessment of drug-induced QT interval prolongation. J Cardiovasc Electrophysiol 2001;12:411–20.
Mehtonen OP, Aranko K, Malkonen L, Vapaatalo H. A survey of sudden death associated with the use of antipsychotic or antidepressant drugs: 49 cases in Finland. Acta Psychiatr Scand 1991;84:58–64.
Mitchell JE, Mackenzie TB. Cardiac effects of lithium therapy in man: a review. J Clin Psychiatry 1982;43:47–51.
Ray WA, Meredith S, Thapa PB, Meador KG, Hall K, Murray KT. Antipsychotics and the risk of sudden cardiac death. Arch Gen Psychiatry 2001;58:1161–7.
Ray, W.A., Chung, C.P., Murray, K.T., Hall, K., Stein, C.M. Atypical antipsychotic drugs and the risk of sudden cardiac death. N Engl J Med 2009;360:225–35.
Reilly JG, Ayis SA, Ferrier IN, Jones SJ, Thomas SH. QTc-interval abnormalities and psychotropic drug therapy in psychiatric patients. Lancet 2000;355:1048–52.
Strachan EM, Kelly CA, Bateman DN. Electrocardiogram and cardiovascular changes in thioridazine and chlorpromazine poisoning. Eur J Clin Pharmacol 2004;60:541–5.
Straus SM, Bleumink GS, Dieleman JP, van der Lei J, t Jong GW, Kingma JH, et al. Antipsychotics and the risk of sudden cardiac death. Arch Intern Med 2004;164:1293–7.
Taggart NW, Haglund CM, Tester DJ, Ackerman MJ. Diagnostic miscues in congenital long-QT syndrome. Circulation 2007;115:2613–20.
Taylor DM. Antipsychotics and QT prolongation. Acta Psychiatr Scand 2003;107:85–95.
The Pfizer 054 study; U.S. Food and Drug Administration Advisory Committee. Zeldox capsules (ziprasidone): summary of efficacy and safety and overall benefit risk relationship. Bethesda, Md: US Food and Drug Administration. Jul 19;2000.
Tschoner A, Engl J, Rettenbacher M, Edlinger M, Kaser S, Tatarczyk T, et al. Effects of six second generation antipsychotics on body weight and metabolism — risk assessment and results from a prospective study. Pharmacopsychiatry 2009;42:29–34.
US Food and Drug Administration Cfdear. Information for healthcare professionals. Haloperidol (marketed as Haldol, Haldol Decanoate and Haldol Lactate). September 17, 2007. http://www.fda.gov/cder/drug/InfoSheets/HCP/haloperidol.htm. Accessed 2008 January 30.
van Noord C, Straus SM, Sturkenboom MC, Hofman A, Aarnoudse AJ, Bagnardi V, et al. Psychotropic drugs associated with corrected QT interval prolongation. J Clin Psychopharmacol 2009;29:9–15.
Vieweg WV. New generation antipsychotic drugs and QTc interval prolongation. Prim Care Companion J Clin Psychiatry 2003;5:205–15.
Vieweg WV, Wood MA, Fernandez A, Beatty-Brooks M, Hasnain M, Pandurangi AK. Proarrhythmic risk with antipsychotic and antidepressant drugs. Implications in the elderly. Drugs Aging 2009;26:997–1012.
Warner JP, Barnes TR, Henry JA. Electrocardiographic changes in patients receiving neuroleptic medication. Acta Psychiatr Scand 1996;93:311–3.
Witchel HJ, Hancox JC, Nutt DJ. Psychotropic drugs, cardiac arrhythmia, and sudden death. J Clin Psychopharmacol 2003;23:58–77.

Biochemical and Biophysical Research Communications 378 (2009) 589–594

Contents lists available at ScienceDirect

Biochemical and Biophysical Research Communications

journal homepage: www.elsevier.com/locate/ybbrc

Evaluation of channel function after alteration of amino acid residues at the pore center of KCNQ1 channel

Taruna Ikrar [a,b], Haruo Hanawa [a], Hiroshi Watanabe [a], Yoshiyasu Aizawa [a,*], Mahmoud M. Ramadan [a], Masaomi Chinushi [a], Minoru Horie [c], Yoshifusa Aizawa [a]

[a] Division of Cardiology, First Department of Internal Medicine, Niigata University Graduate School of Medical and Dental Sciences, 1-754 Asahimachi Dori, Chuo-ku, Niigata 951-8510, Japan
[b] The National Agency for Drug and Food Control, Republic of Indonesia, Jakarta, Indonesia
[c] Department of Cardiovascular and Respiratory Medicine, Shiga University of Medical Science, Shiga, Japan

ARTICLE INFO

Article history:
Received 17 November 2008
Available online 3 December 2008

Keywords:
Long QT syndrome
Missense mutation
KCNQ1
I_{Ks}
Pore center
Amino acid residue

ABSTRACT

The effect of the electrical charge or the size of the amino acid residue at the pore center of a slowly activation component of the delayed rectifier potassium channel: KCNQ1 was studied. K^+ currents were measured after transfection of one of four KCNQ1 mutants: substituting Isoleucine with Lysine, Glutamate, Valine or Glycine and then transfected in COS-7 cells. Both the negatively- and positive charged residue I313 K and I313E showed a loss of function when expressed alone and a dominant negative suppression when co-expressed with wild type KCNQ1. When the site was substituted with the smallest neutral amino acid residue: I313G, there was a small reduction of current when transfected alone and a gain of function when co-transfected with the wild type. I313V showed no difference from the wild type. Changes of amino acid residue at the pore center of KCNQ1 may alter the channel function but this depends on the electrical charge or the size of amino acid residue.

The delayed rectifier K^+ current (I_{Ks}) channel is formed by the co-assembly of KCNQ1 (KvLQT1) with KCNE1 (minK) and contributes to repolarizing cardiac myocytes [1]. A mutation in either subunit is well known to cause long QT syndrome (LQTS) which predisposes affected individuals to cardiac arrhythmias and sudden death [2,3].

In LQTS, the phenotype was suggested to be affected by the site of the mutation and patients with trans-membrane mutations had more frequent diagnostic criteria, LQTS-related cardiac events and a prolonged QT-interval after exercise than patients with a C-terminal mutation [4]. However, this finding from Japan is in contrast to that of the International Long QT Syndrome Registry in which the phenotypes were not related to the site of the mutation [5].

We have previously characterized the physiological consequences of the LQTS-associated mutation at the pore center: I313K, in a patient with a severe LQT1 phenotype [6]. The mutant channels showed almost no current when transfected alone but when co-expressed with WT-KCNQ1, they showed a dominant negative suppression [6].

In this report, our aim was to explore the effects of the charge and the size of the amino acid residue at the pore center of KCNQ1. In order to do this, we substituted its Isoleucine residue with electrically charged ones: Lysine and Glutamate and two neutral amino acids: Valine and Glycine, and performed an electrophysiological study after transfection of each mutant.

Materials and methods

Construction of plasmid DNA for gene transfer. A full-length human WT-KCNQ1, KCNE1, and mutant KCNQ1 were inserted into a plasmid vector pIRES2-EGFP using BamHI restriction sites making the pIRES2-EGFP-KCNQ1, pIRES-EGFP-KCNE1, and mutant pIRES2-EGFP-I313K plasmids as described previously [6]. In the pIRES2-EGFP-I313K plasmid, we introduced three new missense mutations which can occur in humans. One is a mutant with Glutamate which is a positively charged large amino acid residue (I313E). Then we prepared two mutants, Valine (I313V), a neutral amino acid of similar size and homology to the Isoleucine residue in WT-KCNQ1 [7–10] and Glycine as the smallest sized neutral amino acid (I313G).

The mutation of I313E was introduced with a PCR reaction using the mutant primer sets: 5′-GTGGTCACAGTCACCACC*gaa*GGCTATGG GGACAAGGTG-3′ and 5′-CACCTTGTCCCCATAGCC*ttc*GGTGGTGACTG TGACCAC-3′ (*lower case letters indicate mutation sites*). The mutation of I313V was introduced with a PCR using the mutant primer sets 5′-GTGGTCACAGTCACCACC*gtc*GGCTATGGGGACAAGGTG-3′ and 5′-CA CCTTGTCCCCATAGCC*gac*GGTGGTGACTGTGACCAC-3. For the mutation of I313G, we used the primer sets 5′-GTGGTCACAGTCACCA

* Corresponding author. Fax: +81 25 228 5611.
E-mail address: aizaways@med.niigata-u.ac.jp (Y. Aizawa).

0006-291X/$ - see front matter © 2008 Elsevier Inc. All rights reserved.
doi:10.1016/j.bbrc.2008.11.076

CCggcGGCTATGGGGACAAGGTG-3′ and 5′-CACCTTGTCCCCATAGC CgccGGTGGTGACTGTGACCAC-3′.

For these experiments, we used the QuickChange site-directed mutagenesis kit (Stratagene, La Jolla, CA, USA). The resulting products were again amplified by PCR using the primers 5′-CCATTTCCATC ATCGACCTCA-3′ and 5′-AAGGAGAGCGCTGGTGAAG-3′. This final PCR product was ligated to the pIRES2-EGFP WT-KCNQ1 vector using the PstI sites at nucleotide positions 697 and 1675 of KCNQ1. The PCR insert was also cleaved with PstI prior to ligation. The resulting four cloned plasmids were then transformed into *Escherichia coli* JM109 competent cells and purified using a Quantum Prep Plasmid Maxi prep kit (Bio-Rad Laboratories, Hercules, CA).

Culture and transfection of COS-7 cells. A COS-7 monkey kidney cell line was obtained from the American Type Cell Collection and cultured in Dulbecco's modified Eagles medium (Invitrogen Corporation, Gibco-BRL, Rockville, MD) supplemented with 1% penicillin–streptomycin (prepared with 10,000 U/ml penicillin G sodium and 10,000 μg/ml streptomycin sulfate in 0.85% saline) and 10% fetal bovine serum in a humidified 5% CO_2 incubator at 37 °C. The number of cells seeded per ml of medium was 2×10^5 on average. Cultured cells were seeded in 60 mm plates 24 h before transfection, then transiently transfected with various plasmids by the Fugene-6 method (Roche Applied Science, Indianapolis, IN).

Electrophysiological experiments. The whole-cell patch-clamp method was applied to COS-7 cells transfected with the wild type and/or mutant plasmids as described previously [6,11,12]. Briefly, cells were allowed to settle at the bottom of a bath (0.5 ml) mounted on an inverted microscope (Olympus Corp., Tokyo, Japan). Cells were superfused with the bath solution (140 mmol NaCl, 5.4 mmol KCl, 0.5 mmol $MgCl_2$, 1.8 mmol $CaCl_2$, 0.33 mmol NaH_2PO_4, 5.5 mmol glucose and 5 mmol HEPES) and the pH was adjusted to 7.4 by using NaOH. When inserted into the cell/bath solution, a glass pipette with an internal diameter of 1.0–1.5 μm had a resistance of 4–6 MΩ when filled with the following internal solution: 100 mmol/l K-aspartate, 20 mmol/l KCl, 5 mmol/l ATP-Mg, 5 mmol/l phosphocreatine-dipotassium, 5 mmol/l EGTA, 5 mmol/l HEPES and 1 mmol/l $CaCl_2$ (the pH was adjusted to 7.2 with KOH). A patch-clamp amplifier Axopatch 200B (Axon Instruments, Foster City, CA) was used to record membrane currents.

After obtaining a whole-cell configuration, cell membrane capacitance was estimated by analyzing the transient capacitance elicited by 5 mV hyperpolarizing pulses. Cells were held at a starting potential of −80 mV and depolarizing pulses of various potentials ranging from −80 to +80 mV in 20 mV increments for 2 s were applied, followed by repolarization to −40 mV for 2 s to record tail currents. The pCLAMP 8.0 software (Axon Instruments, Foster City, CA) was used to generate the pulse protocol, data acquisition, and analyses.

To be confident of the currents obtained, our analyses only included recordings obtained by Giga-seal after applying the following quality control criteria for the patch-clamp technique [13]: (1) the starting seal resistance was required to be more than 1 GΩ, (2) the series resistance was required to be lower than 20 MΩ throughout the recording, (3) the membrane potential was required to be at a higher negative level than −50 mV if normal high-potassium intracellular solution was used; and (4) cell capacitance and resistance were required to be stable. Furthermore, to check the quality of our findings, COS-7 cells transfected with wild type KCNQ1 were compared with the results of Barhanin et al. [1] and Sanguinetti et al. [15] regarding the properties and biophysical characteristics of the wild type KCNQ1 potassium current.

Data analyses. Analyses of the data were performed with Clampfit 9.1 (Axon Instruments, Foster City, CA) and SPSS for Windows ver.15 (SPSS Inc., Chicago, IL). The time constants for activation and deactivation were determined by fitting the current recordings with a single-exponential function [16]: $f(t) = A_0 + A\,exp(-t/\tau)$ and the voltage dependence of channel activation and deactivation were fitted with the Boltzmann equation: $I = I_{max}/(1 + exp[(V_{1/2} - V)/k])$, where A was current amplitude, τ was the time constant, t was time, I was current amplitude, I_{max} was the maximal tail current, V was the test pulse potential, $V_{1/2}$ was the half-maximal activation potential, and k was the slope of the activation curve. The relationship of current density with side-chain residue volume was measured after 2 s during depolarization.

Results for continuous normal data were expressed as mean ± standard error of estimation. The comparison of means of continuous normal variables across a grouping variable with two levels was done using the student's t-test and the comparison of means of continuous normal variables across a grouping variable with several levels was undertaken with one-way analysis of variance (ANOVA). A two-sided significance level of 0.05 was used for all analyses.

Results

Wild type and mutant channel currents

The cells transfected with KCNQ1 and KCNE1 exhibited a slowly activated outward current compatible with I_{Ks} from native cardiac myocytes. Each mutant was then transfected with KCNE1 and the current–voltage relationships of the peak current during depolarization and the tail current were measured as Fig. 1.

I313 G ($n = 17$ cells) showed an approximately 20% reduction in peak current and the densities of the peak and tail currents were less than those of the wild type ($n = 10$ cells) but the differences were not significant ($P = 0.987$). The activation curve shifted towards the left (Fig. 1A, B, F and Table 1). I313V ($n = 15$ cells) exhibited no significant change in the current compared to those of the wild type ($P = 1.00$, Fig. 1A–C and F). The shape of the membrane potential vs. the current density curve was also similar among cells transfected with the wild type and I313V ($P = 1.00$, Fig. 1F and G).

I313K ($n = 14$ cells) produced almost no current and I313E ($n = 15$ cells) showed a marked reduction of current compared to the wild type ($P < 0.01$ for both, Fig. 1A, D, E and Table 1).

Co-expression of WT and mutant KCNQ1 channels

Cells were then co-transfected with 0.5 μg of each mutant and 0.5 μg of the wild type together with KCNE1 (Fig. 2). Co-transfection of I313 G with the wild type ($n = 16$ cells) showed a 2-fold increase of the current compared to the cells transfected with the wild type: 110.7 ± 4.7 vs. 57.1 ± 6.2 pA/pF ($P < 0.001$) (Fig. 2A and B) and the tail current was also significantly augmented: 26.2 ± 1.7 vs. 16.0 ± 2.3 pA/pF ($P < 0.05$). The activation curve was shifted towards the left (Fig. 2E and F). I313 V co-transfected with the wild type ($n = 9$ cells) showed similar current intensities without significant differences ($P = 1.00$) compared to the wild type ($n = 11$ cells) (Fig. 2A, C and Table 1). Co-transfection of I313E with the wild type ($n = 15$ cells) exhibited a similar current to that of cells co-transfected with I313 K and the wild type ($n = 14$ cells) both showing >70% reduction of current amplitude compared to the wild type ($P < 0.001$) (Fig. 2D–E, and Table 1). An increased current in I313G with the wild type suggested a gain of function and a markedly reduced current in I313E and I313K when co-expressed with the wild type would reflect a dominant negative suppression (Fig. 2F–G).

Kinetic analysis of mutant KCNQ1 channels

The hetero-tetrameric of the wild type and mutant channel in the presence of KCNE1 showed peak and tail currents which were well fitted with the Boltzmann equation or a single-exponential

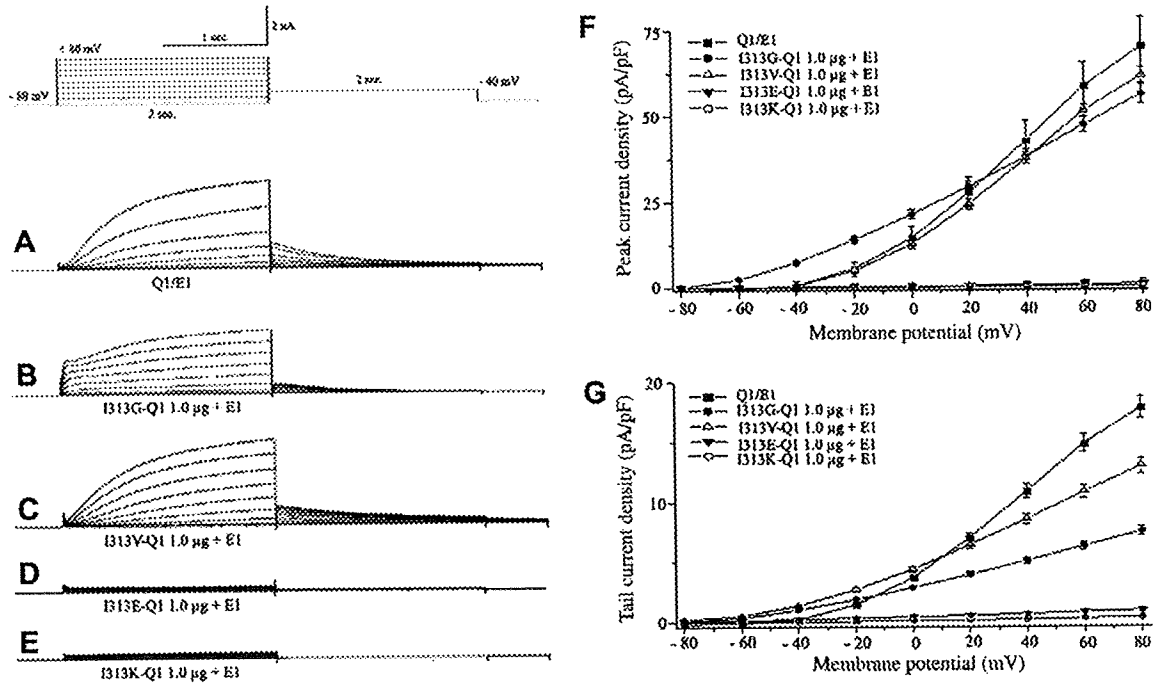

Fig. 1. Results of the whole-cell patch-clamp experiments in COS-7 cells. COS-7 cells were transfected with plasmids of wild type KCNQ1 (Q1) and four mutants together with (E1)KCNE1 (A–E). The activation is rapid but the peak current was about 20% smaller in I313G (B) compared with the wild type (A). I313K and I313E showed almost no current (D,E). The current–voltage relationships of cells transfected with five plasmids are shown on the right and a shift to the left can be seen in I313G (F). The differences in the peak and tail currents among the wild type and four mutants were not significant. Pulse protocol and graph scale are shown at the top.

Table 1
Comparison of kinetics and peak currents in COS-7 cells transfected with wild type and/or mutant KCNQ1 plasmids.

Plasmid DNA	Peak current	Activation curve (mV)		Time constants (τ, ms)	
	(pA/pF)	($V_{1/2}$)	Slope (k)	Activation	Deactivation
WT 1.0 ng (n = 10)	70.4 ± 8.7 2	17.0 ± 1.4	17.0 ± 1.4	1252.0 ± 14.2	2.0 ± 14.2220
I313G 1.0 ng (n = 17)	56.4 ± 2.7[‡]	17.6 ± 1.3[†]	19.9 ± 1.2[†]	607.4 ± 5.2[‡]	397.2 ± 14.5[‡]
I313V 1.0 ng (n = 15)	61.8 ± 2.2[†]	20.9 ± 1.6[†]	17.3 ± 1.1[†]	1389.6 ± 5.7[*]	369.3 ± 110.6[*]
I313E 1.0 ng (n = 15)	0.9 ± 1.1[‡]	–	–	–	–
I313K 1.0 ng (n = 14)	0.4 ± 0.2[‡]	–	–	–	–
WT[#] (n = 11)	57.1 ± 6.2	23.2 ± 1.3	16.7 ± 1.1	1154.3 ± 62.8	213.6 ± 11.85
WT/I313G (n = 16)	110.7 ± 4.7[*]	15.6 ± 1.2[*]	20.2 ± 1.3[*]	350.8 ± 3.0[*]	648.4 ± 126.0[*]
WT/I313V (n = 9)	59.5 ± 1.5[§]	22.5 ± 1.1[§]	16.9 ± 1.0[§]	1297.5 ± 5.7[§]	327.53 ± 110.6[§]
WT/I313E (n = 15)	9.3 ± 0.5[*]	19.0 ± 1.1[§]	18.1 ± 1.0[§]	1242.2 ± 91.4[§]	289.0 ± 74.4[§]
WT/I313K (n = 14)	14.6 ± 1.7[*]	23.9 ± 1.8[§]	17.1 ± 1.6[§]	1302.1 ± 88.2[§]	388.4 ± 64.4[§]

Data represents the mean ± SEM.
WT, wild type; KCNQ1 (α subunit of the potassium voltage-gated channel KQT-like subfamily member 1); KCNE1, β subunit of the potassium voltage-gated channel I_{Ks}-related family member 1; I313K;I313E;I313V and I313G: mutant KCNQ1.
[‡] $P < 0.01$ vs. WT 1.0 μg/KCNE1 1.0 μg.
[†] $P > 0.05$ vs. WT 1.0 μg/KCNE1 1.0 μg.
[#] 0.5 μg of WT was transfected and subsequent study was transfected 0.5 μg of mutant.
[*] $P < 0.001$ vs. WT 0.5 μg/KCNE1 1.0 μg.
[§] $P > 0.05$ vs. WT 0.5 μg/KCNE1 1.0 μg. Each plasmid was transfected with KCNE1 (see text).

function [16]. The activation curves for cells transfected with the wild type and that of co-transfection with I313K, I313E or I313V were not significantly different (Table 1).

Expression of I313G alone showed a more rapid initial activation compared to the wild type: 607.4 ± 5.2 vs. 1252.0 ± 14.2 ms ($P < 0.01$) and smaller $V_{1/2}$: 17.6 ± 1.3 vs. 23.5 ± 1.4 mV ($P < 0.01$) as shown in Fig. 1 and Table 1. I313 G co-transfected with the wild type showed a significant shift in the activation curve towards the left compared with the wild type and the time constant of activation was smaller: 350.8 ± 3.0 vs. 1154.3 ± 62.8 ms ($P < 0.001$) while that of deactivation of the tail current was larger: 648.4 ± 126.0 vs. 213.6 ± 11.85 ms ($P < 0.001$) as shown in Fig. 2A and B, Table 1).

The activation curves for cells transfected with I313E, I313K and I313V together with the wild type revealed statistically non-significant differences compared to cells transfected with the wild type alone ($P = 0.99$, Fig. 2). The time constants were similar among these three mutants but that of I313G was larger at the membrane potential<−25 mV and smaller at >−25 mV (Fig. 3A).

The current density was also affected by the side-chain volume of amino acid residue at position 313 and a significantly larger current density was found only when I313G was co-expressed with the wild type compared with when it was expressed alone (Fig. 3B). Both the homo-tetrameric and hetero-tetrameric I313G

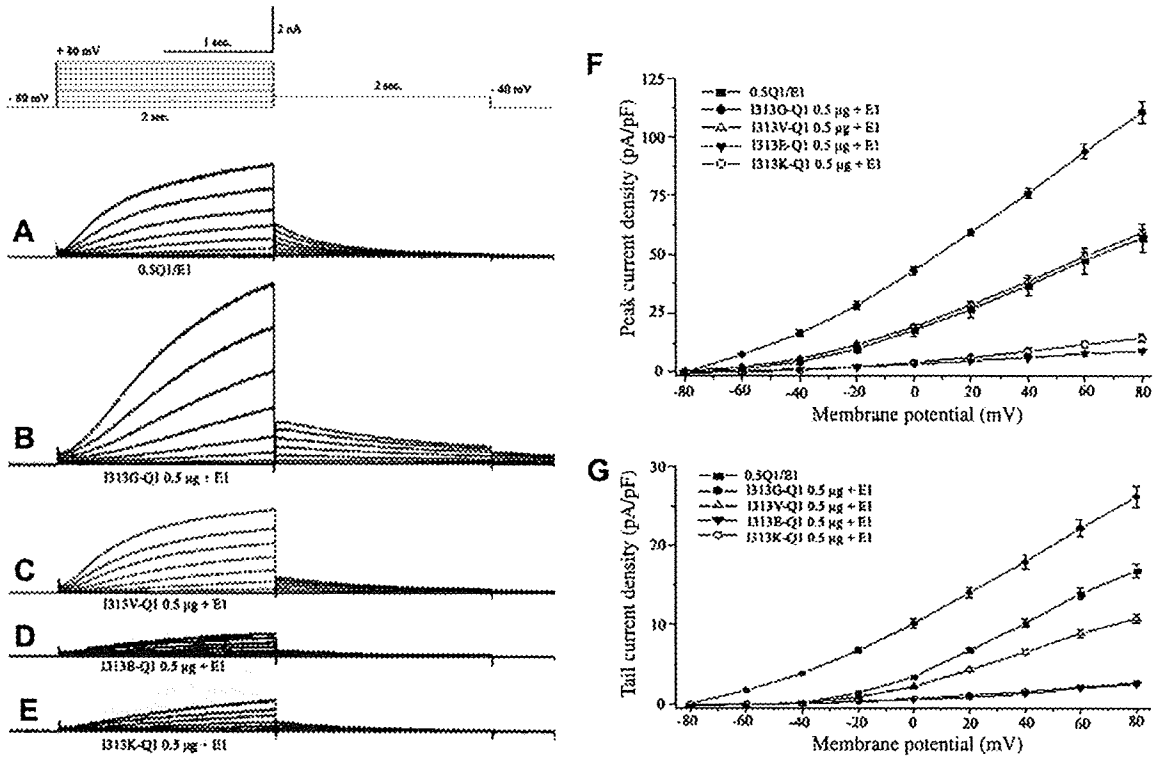

Fig. 2. Results of the whole-cell patch-clamp experiments in COS-7 cells. COS-7 cells were co-transfected with wild type KCNQ1 and four mutants together with KCNE1 (A–E). Current–voltage relationships are shown on the right (F,G). Augmented peak ($P < 0.001$) and tail current ($P < 0.05$) and a shift to the left in activation curve was observed when I313G was co-transfected with the wild type KCNQ1 (B and F). Dominant negative suppression was seen in D and E in which the amino acid residue was replaced by an either positive or negative charged one (D,E). Pulse protocol and graph scale are shown at the top.

with the wild type showed a shift to the left in the activation curve (Fig. 3C) suggesting a altered gating.

Discussion

Both negatively charged (I313K) and positively charged (I313E) residues at the pore center of KCNQ1 resulted in an apparent loss of channel function when they were transfected alone (with KCNE1). The loss of function was not due to a trafficking defect and when they were co-transfected with wild type KCNQ1 (with KCNE1), a dominant negative suppression was observed.

The I_{Ks} channel has six trans-membrane domains (S1–S6), a voltage sensor (S4) and a pore helix selectivity filter segment (P-loop) that connects S5 and S6 [10,17]. The selectivity filter is reflected in a highly conserved amino acid sequence for specific ion conductance as elegantly defined by the crystal structure of the bacterial KcsA channel [18] and the carbonyl oxygen atoms of these residues which bind dehydrated K^+ ions and act for selectivity [19,20]. An altered charge at the pore center, I313K and I313E, is expected to result in a crucial change of the electrostatic environment of the selectivity filter, with serious consequences that reduce the conduction of K^+ ions [21–24]. The presence of charged amino acid residues at the pore center may also disturb the closed/open equilibrium and lead to the destabilization of the open-state of the channel [25] but this was not confirmed in the present study.

The current density was also affected by the side-chain volume of the amino acid residue at the pore center (Fig. 3B and Table 1). When we substituted the neutral Isoleucine residue of KCNQ1 with Valine (I313V) which has a similar size and polarity to Isoleucine, the normalized current–voltage relationship was very similar to the wild type. The homo-tetramer of the Glycine residue (I313G) showed a reduction of the peak K^+ current by about 20% compared with the wild type, but the initial current was larger (Fig. 1B). Furthermore when I313G was co-expressed with the wild type KCNQ1, the K^+ current increased 2-fold which suggests a gain of function (Fig. 2B).

The conductive conformation of the K^+ channel represents a match between the ion-binding sites and the size of K^+ ions [26] and the filter atoms and the surrounding protein atoms are important for selective ion-binding and conduction [9,10]. The volume of side-chain residues located in position 313 may affect conduction of K^+ ions [27].

For the augmented K^+ currents observed in the I313G mutant, we postulate as follows. The homo-tetramer by the smallest amino acid residue Glycine minimized the selectivity filter size (pore) and resulted in a reduced peak current. However, when the mutant was co-transfected with the wild type, the pore was composed of mixed amino acid residue, Glycine and Isoleucine rendered the channel pore larger and augmented the K^+ current (Fig. 3C). Using Brownian dynamics on a simplified model of the KcsA structure, it was shown that altering the pore size of the cytosolic entrance to the selectivity filter led to a change in conductance [28].

As limitations, except for I313K, other mutants are virtual and we have no clinical counterparts so far, but if I313G is associated with short QT syndrome or not is of interest [29]. The change in ion selectivity in each mutant and the relation to the gating mechanism was not fully studied in the present report [30].

As clinical implications, the functional consequences of mutations at the pore center of KCNQ1 varied: from dominant negative suppression to a gain of function when co-transfected with wild type KCNQ1. Severe reduction of I_{Ks} would be detectable as LQTS but a subtle change in K^+ channel function of varying degrees might go undetected.

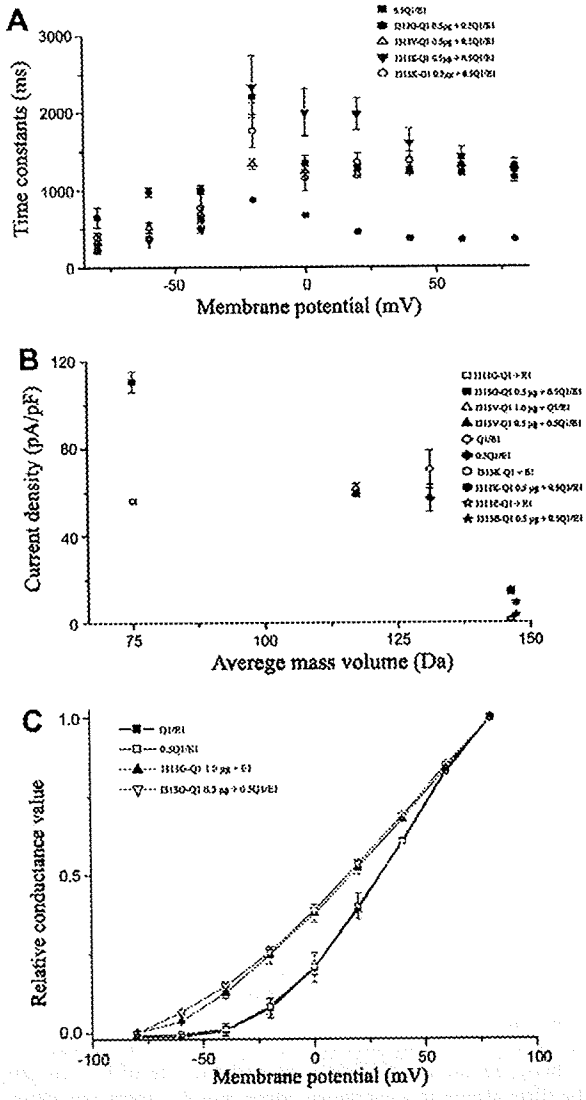

Fig. 3. Activation and deactivation kinetics of currents in the wild type and mutant K^+ channels. In A, activation and deactivation kinetics of co-expression mutants and the wild type KCNQ1 together with KCNE1 are shown. The time constants were derived from the raw current traces and plotted as the function of membrane potential. Substitution of amino acid residue at the pore center (313) altered the relation between the time constant and membrane potential. In B, currents measured at +80 mV and were plotted against the side-chain mass average volume of the residues at position 313 (n = 9–19). The current was least in I313K and I313E but larger when I313G was co-expressed with the wild type. I313V was close to the wild type. In C, relative conductance of the initial tail current amplitude was similar when I313G was transfected alone or with the wild type (+KCNE1). Both shifted toward the left compared to the wild type.

In conclusion, charged residues at the pore center of KCNQ1 resulted in a loss of K^+ channel function and a dominant negative pattern when co-transfected with the wild type channel. The neutral residues showed zero or a small reduction of the K^+ current and some mutants might show a gain of function when co-expressed with the wilt type channel. Not only the site of the mutation but the alteration in charge or size seems to affect phenotype of LQTS.

Acknowledgment

This work was supported by a grant from the Japanese Ministry of Education, Science and Culture, Tokyo, Japan.

References

[1] J. Barhanin, F. Lesage, E. Guillemare, M. Fink, M. Lazdunski, G. Romey, K(V)LQT1 and IsK (minK) proteins associate to form the I(Ks) cardiac potassium current, Nature 384 (1996) 78–80.
[2] A.J. Moss, R.S. Kass, Long QT syndrome: from channels to cardiac arrhythmias, J. Clin. Invest. 115 (2005) 2018–2024.
[3] E. Marban, Cardiac channelopathies, Nature 415 (2002) 213–218.
[4] W. Shimizu, M. Horie, S. Ohno, K. Takenaka, M. Yamaguchi, M. Shimizu, T. Washizuka, Y. Aizawa, K. Nakamura, T. Ohe, T. Aiba, Y. Miyamoto, Y. Yoshimasa, J.A. Towbin, S.G. Priori, S. Kamakura, Mutation site-specific differences in arrhythmic risk and sensitivity to sympathetic stimulation in the LQT1 form of congenital long QT syndrome: multicenter study in Japan, J. Am. Coll. Cardiol. 44 (2004) 117–125.
[5] W. Zareba, J.A. Moss, G. Sheu, E.S. Kaufman, S. Priori, G.M. Vincent, J.A. Towbin, J. Benhorin, P.J. Svhwartz, C. Napolitano, W.J. Hall, M.T. Keating, M. Qi, J.L. Robinsdon, M.L. Andrews, International LQTS registry. Location of mutation in the KCNQ1 and phenotypic presentation of long QT syndrome, J. Cardiovasc. Electrophysiol. 14 (2003) 1149–1153.
[6] T. Ikrar, H. Hanawa, H. Watanabe, S. Okada, Y. Aizawa, M.M. Ramadan, S. Komura, F.Y. amashita, M. Chinushi, Y. Aizawa, A double point mutation in the selectivity filter site of the KCNQ1 potassium channel results in a severe phenotype, LQT1, of long QT syndrome, J. Cardiovasc. Electrophysiol. 19 (2008) 541–549.
[7] D.J. Snyders, Structure and function of cardiac potassium channels, Cardiovasc. Res. 42 (1999) 377–390.
[8] D.M. Roden, Defective ion channel function in the long QT syndrome: multiple unexpected mechanisms, J. Mol. Cell. Cardiol. 33 (2001) 185–187.
[9] S. Berneche, B. Roux, A gate in the selectivity filter of potassium channels, Structure 13 (2005) 591–600.
[10] D.A. Doyle, J.M. Cabral, R.A. Pfuetzner, A. Kuo, J.M. Gulbis, S.L. Cohen, B.T. Chait, R. MacKinnon, The structure of the potassium channel: molecular basis of K^+ conduction and selectivity, Science 280 (1998) 69–77.
[11] Y. Aizawa, K. Ueda, F. Scornik, J.M. Cordeiro, Y. Wu, M. Desai, A. Guerchicoff, Y. Nagata, Y. Iesaka, A. Kimura, M. Hiraoka, C. Antzelevitch, A novel mutation in KCNQ1 associated with a potent dominant negative effect as the basis for the LQT1 form of the long QT syndrome, J. Cardiovasc. Electrophysiol. 18 (2007) 972–977.
[12] Y. Hosaka, H. Nanawa, T. Washizuka, M. Chinushi, F. Yamashita, T. Yoshia, S. Komura, H. Watanabe, Y. Aizawa, Function, subcellular localization and assembly of a novel mutation of KCNJ2 in Andersen's syndrome, J. Mol. Cell. Cardiol. 35 (4) (2003) 409–415. Apr.
[13] A. Molleman, Patch Clamping: An Introductory Guide to Patch Clamp Electrophysiology, John Wiley & Sons, England, 2003. pp. 107–108..
[15] M.C. Sanguinetti, M.E. Curran, A. Zou, J. Shen, P.S. Spector, D.L. Atkinson, M.T. Keating, Coassembly of K(V)LQT1 and minK (IsK) proteins to form cardiac I(Ks) potassium channel, Nature 384 (1996) 80–83.
[16] I.R. Boulet, A.L. Raes, N. Ottschytsch, D.J. Snyders, Functional effects of a KCNQ1 mutation associated with the long QT syndrome, Cardiovasc. Res. 70 (2006) 466–474.
[17] G. Seebohm, N. Strutz-Seebohm, O.N. Ureche, R . Baltaev, A. Lampert, G. Kornichuk, K. Kamiya, T.V. Wuttke, H. Lerche, M.C. Sanguinetti, F. Lang, Differential roles of S6 domain hinges in the gating of KCNQ potassium channels, Biophys. J. 90 (2006) 2235–2244.
[18] A.D. Wei, A. Butler, L. Salkoff, KCNQ-like potassium channels in *Caenorhabditis elegans* conserved properties and modulation, J. Biol. Chem. 280 (2005) 21337–21345.
[19] J.A. Smith, C.G. Vanoye, A.L. George Jr., J. Meiler, C.R. Sanders, Structural models for the KCNQ1 voltage-gated potassium channel, Biochemistry 46 (2007) 14141–14152.
[20] T.W. Allen, A. Bliznyuk, A.P. Rendell, S.H. Kuyucak, The potassium channel: structure, selectivity and diffusion, J. Chem. Phys. 112 (2000) 8191–8204.
[21] J. Aqvist, V. Luzhkov, Ion permeation mechanism of the potassium channel, Nature 404 (2000) 881–884.
[22] S.Y. Noskov, S. Bernèche, B. Roux, Control of ion selectivity in potassium channels by electrostatic and dynamic properties of carbonyl ligands, Nature 431 (2004) 830–834.
[23] Y. Zhou, R. MacKinnon, The occupancy of ions in the K^+ selectivity filter: charge balance and coupling of ion binding to a protein conformational change underlie high conduction rates, J. Mol. Biol. 333 (2003) 965–975.
[24] D. Bichet, M. Grabe, Y.N. Jan, L.Y. Jan, Electrostatic interactions in the channel cavity as an important determinant of potassium channel selectivity, Proc. Natl. Acad. Sci. USA 103 (2006) 14355–14360.
[25] G. Seebohm, P. Westenskow, F. Lang, M.C. Sanguinetti, Mutation of colocalized residues of the pore helix and transmembrane segments S5 and S6 disrupt deactivation and modify inactivation of KCNQ1 K^+ channels, J. Physiol. 563 (2005) 359–368.
[26] S.W. Lockless, M. Zhou, R. MacKinnon, Structural and thermodynamic properties of selective ion binding in a K+ channel, PLoS Biol. 121 (2007) 1079–1088.
[27] L.J. Mullins, An analysis of pore size in excitable membranes, J. Gen. Physiol. 43 (1960) 105–117.
[28] S.H. Chung, T.W. Allen, S. Kuyucak, Conducting-state properties of the KcsA potassium channel from molecular and Brownian dynamics simulations, Biophys. J. 82 (2002) 628–645.

[29] C. Bellocq, A.C. Ginneken, C.R. Bezzina, M. Alders, D. Escande, M.M. Mannens, I. Baró, A.A. Wilde, Mutation in the KCNQ1 gene leading to the short QT-interval syndrome, Circulation 109 (2004) 2394–2397.

[30] T. Lu, A.Y. Ting, J. Mainland, L.Y. Jan, P.G. Schultz, J. Yang, Probing ion permeation and gating in a K^+ channel with backbone mutations in the selectivity filter, Nat. Neurosci. 4 (2001) 239–246.

Adrenergic regulation of the rapid component of delayed rectifier K^+ current: Implications for arrhythmogenesis in LQT2 patients

Dimitar P. Zankov, MD, PhD,* Hidetada Yoshida, MD, PhD,† Keiko Tsuji, MS,* Futoshi Toyoda, PhD,‡ Wei-Guang Ding, MD, PhD,‡ Hiroshi Matsuura, MD, PhD,‡ Minoru Horie, MD, PhD*

*From the *Department of Cardiovascular and Respiratory Medicine, Shiga University of Medical Science, Otsu, Shiga, Japan; †Department of Cardiology, Graduate School of Medicine, Kyoto University, Kyoto, Japan; ‡Department of Physiology, Shiga University of Medical Science, Otsu, Shiga, Japan.*

BACKGROUND KCNH2 gene mutations disrupting rapid component of I_K (I_{Kr}) underlie type 2 congenital long QT syndrome (LQT2). Startled auditory stimuli are specific symptomatic triggers in LQT2, thus suggesting fast arrhythmogenic mechanism.

OBJECTIVE We investigated acute α_{1A}- and cyclic adenosine monophosphate (cAMP)-related β-adrenergic modulation of I_{Kr} in HL-1 cardiomyocytes, wild type (WT)- and 2 LQT2-associated mutant Kv11.1 channels (Y43D- and K595E-Kv11.1) reconstituted in Chinese hamster ovary (CHO) cells.

METHODS I_{Kr} and Kv11.1 currents were recorded using the whole-cell patch-clamp technique and confocal microscopy of HL-1 cardiomyocytes transfected with green fluorescent protein (GFP)-tagged pleckstrin homology domain of phospholipase C-δ_1 visualized fluctuations of membrane phosphatidylinositol 4,5-bisphosphate (PIP_2) content.

RESULTS In HL-1 cardiomyocytes expressing human α_{1A}-adrenoceptor, superfusion with phenylephrine significantly reduced I_{Kr} amplitude, shifted current activation to more positive potentials, and accelerated kinetics of deactivation. Confocal images showed a decline of membrane PIP_2 content during phenylephrine exposure. Simultaneous application of adenylyl cyclase activator forskolin and phosphodiesterase inhibitor 3-isobutyl-1-methylxantine (IBMX) shifted I_{Kr} activation to more negative potentials and decreased tail current amplitudes after depolarizations between +10 and +50 mV. In CHO cells, α_{1A}-adrenoceptor activation downregulated WT-Kv11.1 channels and forskolin/IBMX produced a dual effect. Expressed alone, the Y43D-Kv11.1 or K595E-Kv11.1 channel had no measurable function. However, co-expression of WT-Kv11.1 and each mutant protein evoked currents with loss-of-function alterations but identical to WT-Kv11.1 α_{1A}- and forskolin/IBMX-induced regulation.

CONCLUSION Acute adrenergic regulation of at least 2 Kv11.1 mutant channels is preserved as in WT-Kv11.1 and native I_{Kr}. Suppression of α_{1A}-adrenoceptor-related transduction might have therapeutic implications in some cases of LQT2.

KEYWORDS Long QT syndrome; I_{Kr}; KCNH2 mutation; α_{1A}-adrenoceptor; β_1- and β_2-adrenoceptor.

(Heart Rhythm 2009;6:1038–1046)

Introduction

Sympathetic activation and arrhythmogenesis are uniquely associated in long QT (LQT) syndrome, the disease that prolongs cardiac repolarization and leads to syncope and sudden cardiac death.[1] This is particularly the case in the most frequent variants, LQT type 1 (LQT1) and type 2 (LQT2), designating malfunction of slowly (I_{Ks}) and rapidly (I_{Kr}) activating components of I_K, respectively. Symptomatic triggers in congenital LQT are gene specific: often after continuous physical exercise (swimming) in LQT1 and startled auditory stimuli in LQT2.[2,3]

Efficiency of β-blocker therapy in LQT tends to divert attention from possible α_{1A}-adrenoceptor (α_{1A}AR)-mediated arrhythmogenic mechanisms. Increase of action potential duration (APD) in Purkinje fibers by α_{1A}AR stimulation is well-documented phenomenon that would promote arrhythmogenesis in LQT.[4,5] Moreover, between 36% and 41% of patients with LQT2 (focus of this report) are resistant to β-blockers,[2,6] and the efficacy of combined α_1- and β-blockers (e.g., labetalol) in some of the LQT cases has been reported.[7]

I_{Kr} or Kv11.1 (reconstituted α-subunit of human I_{Kr} channel) current inhibition by the selective α_{1A}AR agonist phenylephrine was found in Xenopus oocyte[8,9] mammalian cell lines and rabbit ventricular myocytes.[10,11] β_1- and β_2 adrenoceptors ($\beta_{1,2}$AR) modulate I_{Kr} through the dual action of cyclic adenosine monophosphate (cAMP): direct binding to the I_{Kr} channel produces a hyperpolarizing shift

This study was supported by the Japanese Society for the Promotion of Science, research grant No. 19-07209. **Address reprint requests and correspondence:** Dr. Minoru Horie, Department of Cardiovascular and Respiratory Medicine, Shiga University of Medical Science, Otsu, Shiga 520-2192, Japan. E-mail address: horie@belle.shiga-med.ac.jp. (Received December 20, 2008; accepted February 25, 2009.)

1547-5271/$ -see front matter doi:10.1016/j.hrthm.2009.02.045

of current activation, and stimulation of protein kinase A (PKA) results in I_{Kr} inhibition.[12,13] The net effect varies according to different reports.[14,15]

Startled auditory stimuli-triggered syncope in LQT2 suggests involvement of fast transduction. Therefore, we studied immediate α_{1A} and $\beta_{1,2}$AR regulation of I_{Kr} in HL-1 cardiomyocytes,[16] wild-type (WT)-Kv11.1 current in Chinese hamster ovary (CHO) cells, and 2 Kv11.1 mutant channels (Y43D-Kv11.1 and K595E-Kv11.1) found in LQT2 probands with loud noise–triggered syncope.

Methods

Cell lines

HL-1 cardiomyocytes, a generous gift from Dr W. C. Claycomb, Louisiana State University Health Sciences Center, New Orleans, Louisiana, derived from AT-1 cells.[16] They retain differentiated cardiac phenotype during indefinite passages in culture, generate spontaneous action potentials, and express various ion channels characteristic for mouse atrium.[16,17]

The cells were cultured as originally described[16] and transiently co-transfected with 1 μg human α_{1A}AR/pcDNA3.1 + (Missouri S&T cDNA Resource Center, Rolla, Missouri) and 0.5 μg pEGFP (Invitrogen, Carlsbad, California) or 1 μg PH-GFP/pCI (Promega, Madison, Wisconsin), using Lipofectamin 2000 Reagent (Invitrogen). After transfection with α_{1A}AR, HL-1 cardiomyocytes were kept in norepinephrine-free medium to avoid desensitization of reconstituted α_{1A}AR.

CHO cells were cultured as reported previously.[18] WT-Kv11.1/pRC (Invitrogen), Y43D-Kv11.1 or K595E-Kv11.1/pRC, each 1 μg, were co-transfected with 0.5 μg pEGFP and 1 μg human α_{1A}AR using Lipofectamin Reagent (Invitrogen). In the subset of experiments, 1 μg Y43D-Kv11.1 or K595E-Kv11.1 were co-transfected with WT-Kv11.1 (1 μg), human α_{1A}AR (1 μg), and pEGFP (0.5 μg) cDNA. WT-Kv11.1 cDNA was a generous gift from Dr M. C. Sanguinetti, Nora Eccles Harrison Cardiovascular Research and Training Institute, University of Utah, Salt Lake City, Utah.

Kv11.1 mutations

Among the LQT2-associated mutations identified in our institution, we selected 2 novel heterozygous KCNH2 mutations from probands with auditory stimuli-induced symptoms.

Y43D-Kv11.1.

A 30-year-old woman had experienced repetitive syncope since the age of 13. The attacks had been provoked by sudden arousal, e.g., ringing telephone during sleep and never by exercise. Electrocardiogram at rest showed corrected QT interval (QTc) of 0.60 seconds (Bazett formula). α_1- and β-adrenergic blocker carvedilol (20 mg/day) terminated the syncope completely.

K595E-Kv11.1.

A 35-year-old woman has had syncopal attacks since her infancy. Torsades de pointes was documented at the age of 18, and propranolol (40 mg/day) was administered but ineffective. Multiple episodes of syncope recurred after sudden arousal or auditory stimulation, although her QTc was not so prolonged (0.47 seconds) in the presence of propranolol. An implantable cardioverter-defibrillator was then implanted.

Electrophysiological experiments

I_{Kr} and Kv11.1 currents were measured at 37°C using the standard whole-cell patch-clamp technique[19] with EPC-8 amplifier (HEKA, Lambrecht, Germany) and 2.5 to 3.5 MΩ glass electrodes. Series resistance (maximally approximately 8 MΩ) was not compensated, and leak subtraction was not performed. Liquid junction potential between normal Tyrode and intracellular solution (−10 mV) was corrected in the data.

I_{Kr} was elicited by 2-second depolarizations from holding potential of −50 mV (to inactivate sodium, transient outward potassium, and T-type calcium currents) followed by repolarizations to the holding potential to record tail currents. L-type calcium current was eliminated by addition of 0.4 μmol/l nisoldipine to the external solution. We were not able to detect HMR1556-sensitive current in HL-1 cardiomyocytes (I_{Ks}, data not shown), and I_{Ks} blocker was not used. Kv11.1 current in CHO cells was evoked from holding potential −70 mV by 2-second depolarizations and tails were recorded at repolarizing steps between −120 and −20 mV.

Composition of pipette solution was (in mmol/l): 70 potassium aspartate, 50 KCl, 10 KH_2PO_4, 1 $MgSO_4$, 3 Na_2-ATP, 0.1 Li_2-GTP, 5 EGTA and 5 HEPES; pH adjusted to 7.2 with KOH. External solution, normal Tyrode, contained (in mmol/l): 140 NaCl, 5.4 KCl, 1.8 $CaCl_2$, 0.5 $MgCl_2$, 0.33 NaH_2PO_4, 5.5 glucose, and 5.0 HEPES; pH adjusted to 7.4 with NaOH. E-4031 (Wako, Japan), phenylephrine, 3-isobutyl-1-methylxantine (IBMX), and forskolin (Sigma, St. Louis, Missouri) were supplemented into external solution on the day of experiments diluting the necessary amount of stock solutions. Stock solutions (kept at −20°C) of E-4031 and phenylephrine were made in distilled water; IBMX and forskolin were stored in dimethyl sulfoxide. L-α-phosphatidyl-D-myo-inositol-4,5-bisphosphate (PIP_2, Calbiochem, San Diego, California) was added to the pipette solution to achieve concentration of 10 μmol/l and 5 ml aliquots were kept at −80°C maximally for 1 month.

Confocal microscopy

HL-1 cardiomyocytes constantly superfused with normal Tyrode solution at 37°C were examined in the recording chamber of a Zeiss LSM 510 confocal laser-scanning inverted microscope (Carl Zeiss, Oberkochen, Germany). A switch to a phenylephrine-containing (30 μmol/l) normal Tyrode solution tested the effect of α_{1A}AR stimulation on GFP-tagged pleckstrin homology domain of phospholipase C-δ_1 (PH-GFP) fluorescence. Confocal images were taken at 15- or 30-second time intervals, and fluorescence intensity was analyzed through the measurement of green plane intensity of the images in ImageJ software (Rasband, W. S.,

ImageJ, National Institutes of Health, Bethesda, Maryland; http://rsb.info.nih.gov/ij/, 1997–2008).

Statistical analysis

All averaged values are presented as mean ± SEM. Statistical comparisons were made by 2-tailed paired and unpaired Student *t*-test or 1-way ANOVA and differences were accepted as significant for $P < .05$.

Results

Stimulation of α_{1A}AR downregulated I_{Kr}

In HL-1 cardiomyocytes expressing human α_{1A}AR, I_{Kr} possessed typical properties as described for the rapid component of I_K.[20] Selective α_{1A}AR agonist phenylephrine, applied externally for 4 to 6 minutes at a concentration of 30 μmol/l, reduced quickly I_{Kr} amplitude, and the readministration of drug-free solution restored the current amplitude to 90% ± 6% (n = 8) of the control level (Figure 1A). Figure 1B shows typical I_{Kr} traces evoked by voltage commands between −40 and +50 mV before and during superfusion with 30 μmol/l phenylephrine, and in the presence of specific I_{Kr} inhibitor E-4031 (3 μmol/l). I_{Kr} block unmasked an existence of endogenous time-independent conductance present during depolarizing steps but not at holding potential. For accurate measurement of I_{Kr} amplitude, we used tail currents because after their complete inhibition by E-4031 no evident time-dependent conductance at −50 mV could be observed. Phenylephrine downregulated I_{Kr} in a voltage-dependent manner: inhibition of I_{Kr} tails varied from 0.68 ± 0.07 at −30 mV to 0.30 ± 0.01 at +50 mV (n = 9, $P < .05$, Figure 1C).

In addition to the reduction of current amplitude, α_{1A}AR stimulation modified I_{Kr} channel gating and facilitated the process of deactivation. The voltage at half-maximal activation ($V_{1/2}$) was shifted toward positive potentials, and fast and slow time constants of deactivation decreased in the presence of phenylephrine (Table 1, Figures 1D to 1F).

The α_{1A}AR modulation of I_{Kr}, evaluated as E-4031 sensitive current, was verified using a ventricular action potential clamp technique. Typical current traces (average of 5 consecutive recordings at steady state) are shown in Figure 2A. Similar to square depolarizations, α_{1A}AR-related decline of E-4031-sensitive current was voltage dependent: the range of measured current inhibition during action potential voltage clamp was between 0.35 at −50 mV and 0.20 at +30 mV (n = 7, $P < .05$, Figure 2B).

Fluctuation of PIP_2 content during α_{1A}AR activation

Variation of membrane PIP_2 concentration could be successfully shown by a method that takes advantage of high-affinity binding of pleckstrin homology domain of PLC-δ_1 (PH) to PIP_2.[21] Expression of GFP-tagged PH could be seen as predominantly cell-membrane-localized fluorescence under the microscope. The decrease of the membrane PIP_2 amount produces a decrease of membrane and an increase of cytosolic fluorescence because of redistribution of PH-GFP.

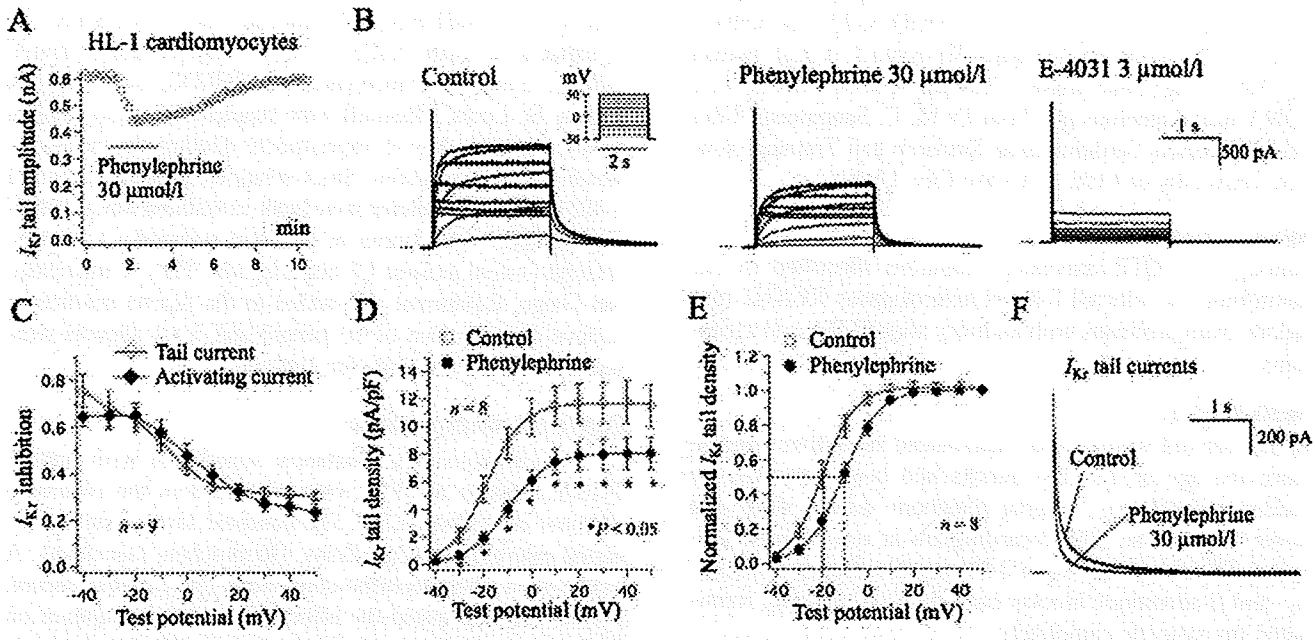

Figure 1 α_{1A}AR agonist phenylephrine downregulated I_{Kr} in HL-1 cardiomyocytes. **A:** Typical time course of I_{Kr} tail amplitudes when cells were exposed to 30 μmol/l phenylephrine: the current decreased quickly after α_{1A}AR stimulation. **B:** Line of control I_{Kr} currents, traces during α_{1A}AR stimulation, and conductance remaining after complete I_{Kr} inhibition by E-4031 (voltage-clamp protocol is in the inset). I_{Kr} suppression was more potent at negative potentials (**C**). **D:** Mean values of I_{Kr} tail densities before and during α_{1A}AR stimulation are plotted against the depolarizing voltages and fitted to the Boltzmann equation. The positive shift of I-V curve was shown when current densities were normalized to the maximal value (**E**). α_{1A}AR stimulation also accelerated I_{Kr} deactivation (Table 1). **F:** Typical tail currents recorded at −50 mV before and after α_{1A}AR stimulation.

Table 1 Activation and deactivation parameters of I_{Kr} in HL-1 cardiomyocytes and Kv11.1 currents in CHO cells

	Control	Phenylephrine	Control	Forskolin/IBMX
I_{Kr}				
$V_{1/2}$ (mV)	−18.7 ± 0.3	−9.9 ± 0.2* (8)†	−18.3 ± 1.3	−21.5 ± 1.1* (17)
k (mV)	+8.4 ± 0.1	+7.6 ± 0.2 (15)	+7.1 ± 0.3	+7.3 ± 0.4 (17)
τ_{fast} (ms)‡	60 ± 17	46 ± 19* (6)	47 ± 15	45 ± 16 (12)
τ_{slow} (ms)‡	586 ± 161	442 ± 212* (6)	451 ± 97	433 ± 107 (12)
Kv11.1 (WT)				
$V_{1/2}$ (mV)	−16.2 ± 0.6	−9.3 ± 0.3* (15)†	−16.4 ± 2.0	−20.9 ± 2.6* (10)
k (mV)	+7.5 ± 0.5	+8.7 ± 0.2 (15)	+8.2 ± 0.5	+8.1 ± 0.5 (10)
τ_{fast} (ms)‡	282 ± 17	205 ± 17* (8)	235 ± 24	224 ± 29 (8)
τ_{slow} (ms)‡	1,570 ± 104	875 ± 96* (8)	1,374 ± 119	1,293 ± 121 (8)
Kv11.1 (WT/Y43D)				
$V_{1/2}$ (mV)	−9.6 ± 0.5	−4.5 ± 0.3* (13)	−13.1 ± 2.1	−20.2 ± 1.6* (11)
k (mV)	+7.4 ± 0.4	+8.6 ± 0.2 (13)	+7.6 ± 0.3	+7.4 ± 0.2 (11)
τ_{fast} (ms)‡	129 ± 8	89 ± 7* (8)	166 ± 26	157 ± 18 (8)
τ_{slow} (ms)‡	642 ± 55	577 ± 48* (8)	810 ± 92	803 ± 100 (8)
Kv11.1 (WT/K595E)				
$V_{1/2}$ (mV)	−5.5 ± 0.6	0.09 ± 0.7* (9)	−3.3 ± 1.8	−8.6 ± 2.2* (11)
k (mV)	+7.5 ± 0.5	+8.6 ± 0.6 (9)	+6.6 ± 0.2	+6.5 ± 0.3 (11)
τ_{fast} (ms)‡	306 ± 32	225 ± 25* (8)	305 ± 37	301 ± 31 (9)
τ_{slow} (ms)‡	1,790 ± 162	1,184 ± 146* (8)	1,582 ± 111	1,577 ± 132 (9)

CHO = Chinese hamster ovary; IBMX = 3-isobutyl-1-methylxantine; WT = wild-type.
*P <.05 vs. control value.
†Figures in parentheses indicate the number of experiments.
‡Shown are the average values of deactivation at −50 mV for I_{Kr} and at −60 mV for Kv11.1 currents.

We used this technique to show the coupling of reconstituted human α_{1A}AR to G_q–PLC pathway. In HL-1 cardiomyocytes co-transfected with PH-GFP and α_{1A}AR cDNA (Figure 3A), phenylephrine caused rapid translocation of the fluorescence from the cell membrane to the cytoplasm (quantitatively analyzed in Figures 3B and 3C). On the contrary, in HL-1 cardiomyocytes expressing only PH-GFP, the membrane and cytosolic fluorescence were not altered by phenylephrine administration (not shown). The average ratio between green plane intensity in the images from cytosolic regions of interest measured in 7 HL-1 cardiomyocytes expressing α_{1A}AR and PH-GFP compared with the value from 4 cardiomyocytes transfected only with PH-GFP equaled 1.27 ± 0.06 and 0.99 ± 0.001, respectively (P <.05 between groups). The above results confirmed coupling between reconstituted human α_{1A}-AR and intracellular pathways.

In the system of HL-1 cardiomyocytes, the molecule responsible for I_{Kr} regulation through α_{1A}AR seemed to be PIP_2. When 10 μmol/l PIP_2 was loaded through the glass electrode (Figure 3D) I_{Kr} tail inhibition after α_{1A}AR activation was largely attenuated (e.g., reduction of mean tail amplitude after depolarization to +30 mV decreased from 31.1% to 11.5%, P <.05) and the phenylephrine-induced shift of I-V curve was only +4.2 mV (compared with +8.8 mV in the control state, P <.05). Deactivation time con-

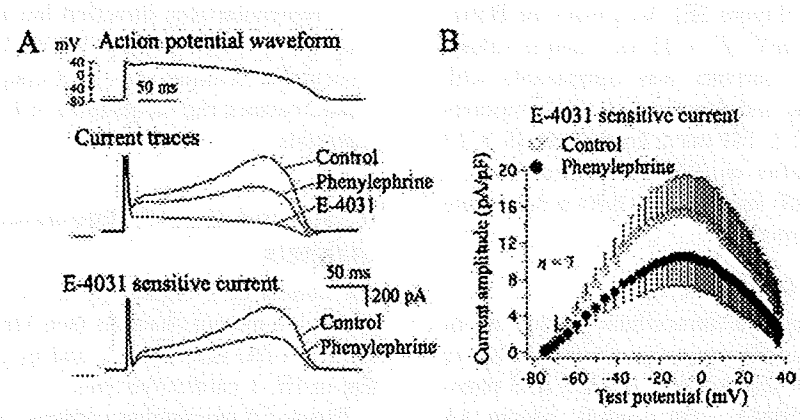

Figure 2 α_{1A}AR activation inhibited I_{Kr} during action potential voltage clamp. I_{Kr} was evoked by voltage-clamp command with ventricular action potential form (**A, top**) to confirm α_{1A}AR-related modulation during physiological variation of membrane potential. Reduction of recorded current by phenylephrine (30 μmol/l) and selective I_{Kr} inhibitor E-4031 (3 μmol/l) is shown (**A, middle**). The trace in the presence of E-4031 was subtracted from the remaining 2 to show E-4031-sensitive current (I_{Kr}) before and during α_{1A}AR stimulation (**A, bottom**). **B**: Average I-V relations of E-4031-sensitive current are presented. The corresponding points are statistically different at potentials more positive than −70 mV (arrow).

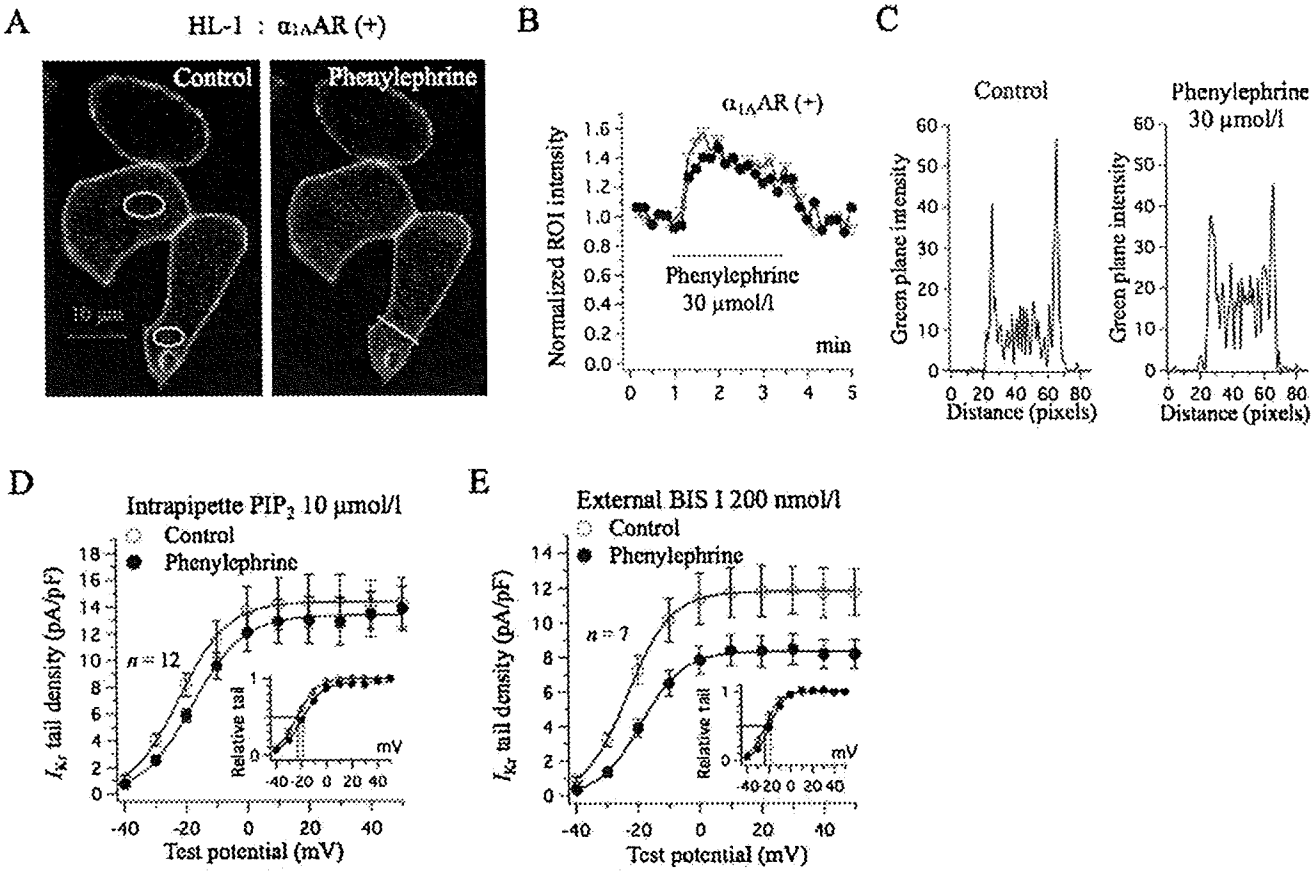

Figure 3 α_{1A}AR-induced depletion of membrane PIP_2 downregulated I_{Kr}. A: Confocal images from HL-1 cardiomyocytes expressing PH-GFP and α_{1A}AR. The fluorescence was located mainly in the cell periphery (membrane), and the signal from the cytosol intensified when external solution contained 30 μmol/l phenylephrine. This effect was quantified by exploring the green plane intensity of region of interests (ROI) and profile across the line (**B, C**), thus confirming functionality of reconstituted human α_{1A}AR. **D:** The mean I_{Kr} tail amplitudes (fitted to the Boltzmann equation) from 12 cardiomyocytes loaded with 10 μmol/l PIP_2 before and during α_{1A}AR stimulation. Inset illustrates the same relation when average tail amplitudes are normalized to the maximal value. Intrapipette PIP_2 significantly diminished phenylephrine-induced I_{Kr} reduction (see text). **E:** On the other hand, specific protein kinase C inhibitor BIS I (200 nmol/l) did not affect extensively I_{Kr} modulation: degree of tail inhibition, positive shift of activation, and facilitation of deactivation were similar to that in the control state.

stants were affected as in the absence of PIP_2 (not shown). On the contrary, the I_{Kr} response to phenylephrine remained identical in the presence of protein kinase C inhibitor bisindolylmaleimide I (BIS I) (Figure 3E): $V_{1/2}$ from the Boltzmann fit increased +5.3 mV ($P > .05$ vs. control value), average reduction of tail currents was comparable with control at all test voltages, and deactivation time constants were 53 ± 16 ms and 540 ± 191 ms in control vs. 35 ± 13 ms and 323 ± 169 ms after α_{1A}AR stimulation (n = 7, $P < .05$). BIS I (200 nmol/l) itself did not have a noticeable effect on control I_{Kr} amplitude.

cAMP-induced modulation of I_{Kr}

We stimulated $\beta_{1,2}$AR-coupled intracellular production of cAMP by exposing HL-1 cardiomyocytes simultaneously to adenylyl cyclase activator (forskolin, 5 μmol/l) and phosphodiesterase inhibitor (IBMX, 100 μmol/l). Figure 4A shows typical I_{Kr} traces in the absence and presence of forskolin/IBMX. Activation of transduction pathways coupled to $\beta_{1,2}$AR had a dual effect on I_{Kr}. Tail amplitudes increased by 43.3% to 7.1% after depolarizations between −50 and −30 mV (Figure 4B) but decreased by 4.1% to 5.5% after depolarization between +20 and +50 mV ($P < .05$). Combination forskolin/IBMX shifted I_{Kr} activation in a hyperpolarizing direction but did not affect considerably deactivation kinetics (Table 1). Thus in HL-1 cardiomyocytes, activation of $\beta_{1,2}$AR-coupled pathways tended to counterbalance the modulation of I_{Kr} by α_{1A}AR at negative potentials.

α_{1A}AR and $\beta_{1,2}$AR regulation of Kv11.1 channels

We investigated regulation of WT-Kv11.1 and 2 LQT2-associated mutant channels (see Methods section) reconstituted in CHO cells by α_{1A} and $\beta_{1,2}$AR in a way similar to that in HL-1 cardiomyocytes.

Figure 5A exemplifies currents recorded from CHO cells co-expressing WT-Kv11.1 and human α_{1A}AR in the control state and during exposure to 30 μmol/l phenylephrine. The α_{1A}AR agonist decreased I_{Kr} tail amplitude, shifted the midpoint of I-V relation rightward, and facilitated deactiva-

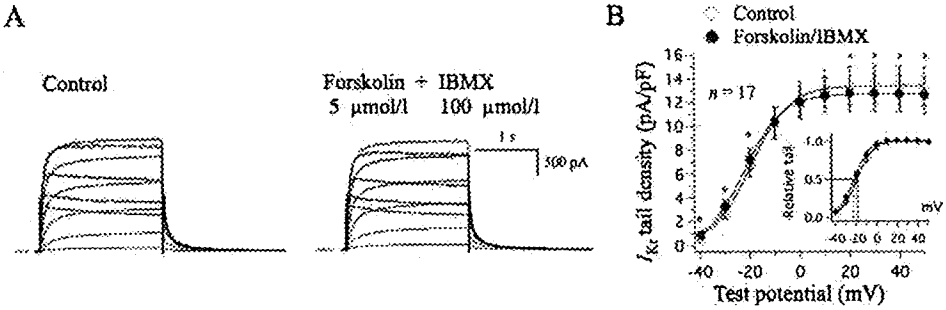

Figure 4 I_{Kr} modulation by $\beta_{1,2}$AR-coupled transduction. **A:** Typical I_{Kr} in HL-1 cardiomyocytes elicited by square voltage-clamp pulses (like in Figure 1B) in control state and during elevation of intracellular cAMP by 5 μmol/l forskolin and 100 μmol/l IBMX. **B:** I_{Kr} tail densities from 17 cells as a function of depolarizing voltage before and during forskolin/IBMX application. Smooth curves (fit to the Boltzmann equation) show −3.2 mV hyperpolarizing shift of I-V relation caused by the drugs (inset). Tail amplitudes were affected significantly after depolarizations between −40 mV and −20 mV (increased) and between +20 and +50 mV (reduced, $*P < .05$).

tion (Figures 7A and 7B). Activation of $\beta_{1,2}$AR-coupled signaling in CHO cells[18] with external forskolin/IBMX had dual effect on tail amplitude as in Figure 4B and shifted current activation to more negative potentials (Figure 5B, Table 1).

Expressed alone, mutant proteins Y43D-Kv11.1 and K595E-Kv11.1 did not produce functional channels (not shown). Co-expression with WT-Kv11.1 generated currents with loss-of-function properties. For WT/Y43D-Kv11.1, a positive shift (+6.6 mV, $P < .05$) of I-V relation and considerable acceleration of deactivation kinetics (Figures 6A, 7C, and 7D); for WT/K595E-Kv11.1, an even more prominent rightward shift of I-V relation (+10.7 mV, $P < .05$) and reduced I_{Kr} amplitude (between 82.5% at −30 mV and 49.3% at +50 mV, $P < .05$, Figure 6C). Nevertheless, stimulation of α_{1A}AR caused additional inhibition of the WT/Y43D-Kv11.1 and WT/K595E-Kv11.1 currents: $V_{1/2}$ was further increased with +5.1 and +5.6 mV, respectively, and time constants of deactivation had diminished values in the course of phenylephrine superfusion (Figures 6A, 6C, and 7C to 7F, Table 1). Forskolin/IBMX modulated both mutant currents similar to WT-Kv11.1: a negative shift of I-V relation and inhibition of tail amplitudes after positive depolarization for WT/Y43D-Kv11.1; a negative shift of the I-V curve for WT/K595E-Kv11.1 (Figures 6B and 6D, Table 1).

Taken together, both studied mutant currents retained regulation by α_{1A}AR and forskolin/IBMX comparable to that of WT-Kv11.1 channels.

Discussion

Acute adrenergic regulation of I_{Kr} and Kv11.1 channels

The main findings in this study can be summarized as follows. α_{1A}AR stimulation downregulated I_{Kr} and reconstituted WT-Kv11.1 channels by decreasing current amplitudes, creating a positive shift of I-V relations, and accelerating deactivation kinetics. The $\beta_{1,2}$AR-associated cAMP increase had dual action on I_{Kr} and Kv11.1: a negative shift of the I-V curves (augmenting the currents at negative potentials) and a decline of current amplitudes at positive

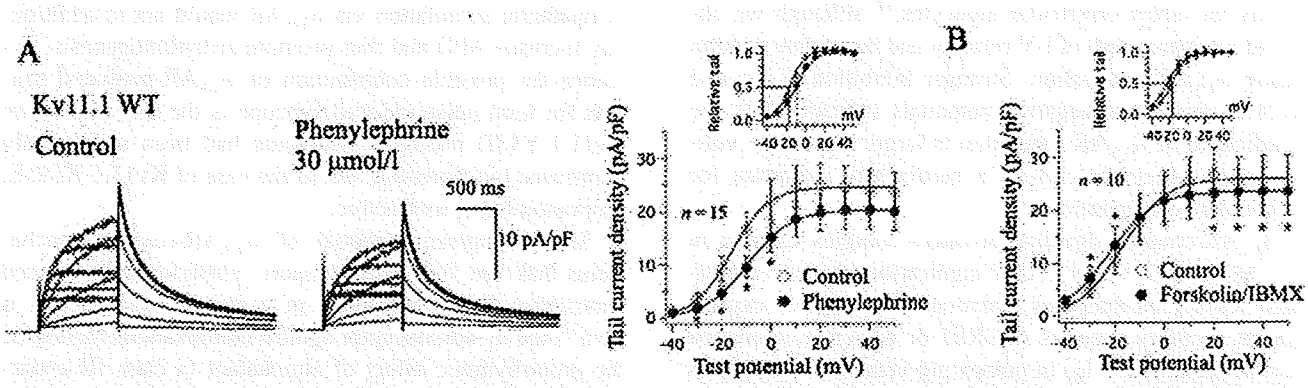

Figure 5 α_{1A}AR and $\beta_{1,2}$AR regulation of reconstituted WT-Kv11.1 channels. **A:** WT-Kv11.1 currents and average I-V relation of WT-Kv11.1 tails density (fitted to the Boltzmann equation) before and during exposure of CHO cells to 30 μmol/l phenylephrine are shown. α_{1A}AR stimulation reduced WT-Kv11.1 tail amplitudes significantly after depolarizations between −30 and 0 mV ($*P < .05$, maximal inhibition was 50.8% after −30 mV), shifted I-V curve in a rightward direction (+6.9 mV), and accelerated deactivation kinetics. Inset shows the mean amplitudes of WT-Kv11.1 tails normalized to the value after +40 mV step. **B:** The combination forskolin/IBMX shifted I-V curve to more negative potentials (−4.5 mV, $*P < .05$), significantly reduced tail amplitudes after depolarizations between +20 and +50 mV (8.0% to 13.6%), and increased tails after depolarizations to −30 and −20 mV (47.6% and 22.2%, respectively).

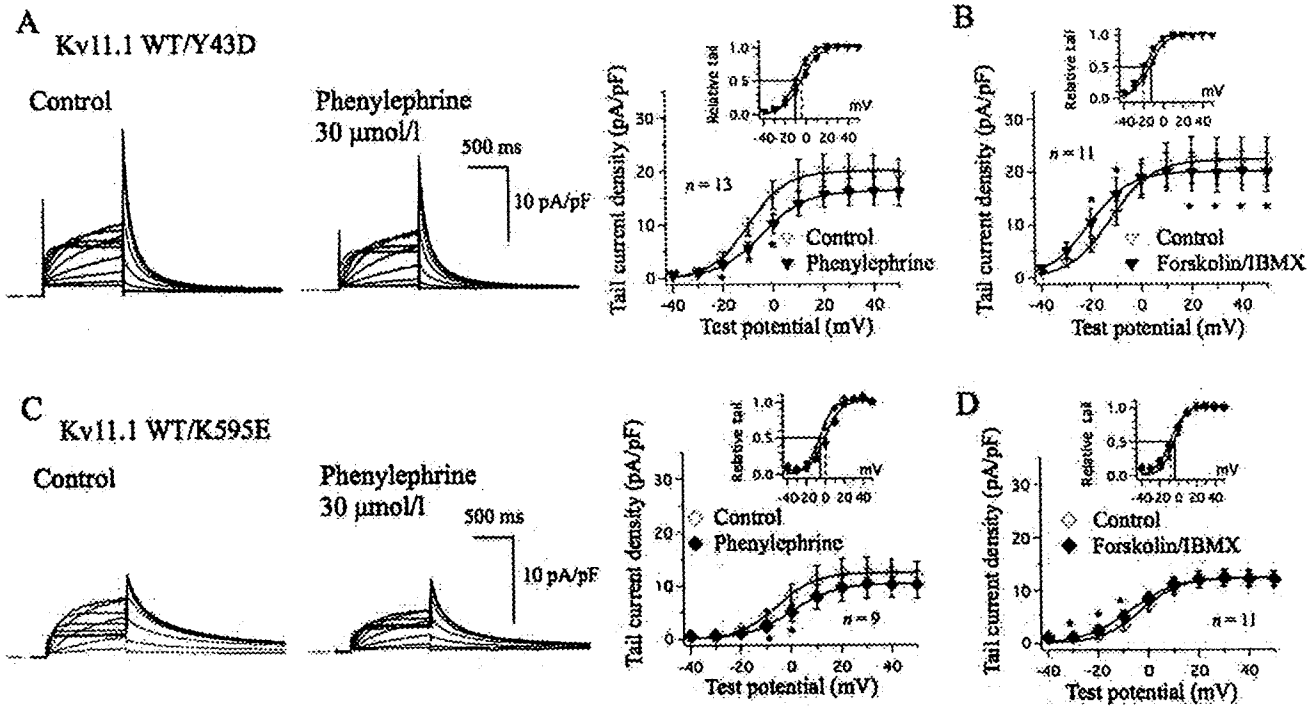

Figure 6 α_{1A}AR and $\beta_{1,2}$AR regulation of WT/Y43D- and WT/K595E-Kv11.1 channels. Phenylephrine and forskolin/IBMX effects on WT/Y43D-Kv11.1 (**A, B**) and WT/K595E-Kv11.1 (**C, D**) currents are presented identically to WT-Kv11.1 in Figure 5. These already deficient mutant channels were additionally downregulated by phenylephrine through inhibition of current amplitude, maximally after −10 mV depolarization (41.2% and 43.8% for WT/Y43D-Kv11.1 and WT/K595E-Kv11.1, respectively, $*P < .05$), positive shift of I-V relation and facilitation of deactivation. Forskolin/IBMX treatment changed the midpoint of I-V curves toward negative potentials for both mutants (Table 1). Forskolin/IBMX reduced the amplitude of WT/Y43D-Kv11.1 tail currents by 8.6% to 10.1% after steps between +20 and +50 mV and augmented tail amplitudes by 71.1% and 28.5% after depolarizations to −20 and −10 mV, respectively. **D**: WT/K595E-Kv11.1 tails increased by 99.0% to 52.6% after test voltages between −30 and −10 mV ($*P < .05$).

potentials. Moreover, 2 mutant channels found in LQT2 probands with loud noise-triggered syncope preserved the same pattern of acute adrenergic regulation.

α_{1A}AR-related modulation of I_{Kr} in ventricular myocytes[11] or Kv11.1 channels in expression systems[8,10] was shown. However, intracellular signaling linking α_{1A}AR and I_{Kr} channels is not sufficiently clarified because conflicting data have been published.[8,10] Our results are close to the reports for rabbit ventricular myocytes,[11] although we observed a positive shift of I-V relation and faster deactivation during α_{1A}AR stimulation. Stronger inhibition of I_{Kr} and Kv11.1 currents at negative potentials indicates that the significance of α_{1A}AR regulation is larger within the voltage range where the current is particularly important for ventricular repolarization.

$\beta_{1,2}$AR-coupled signaling produces complex changes in I_{Kr}: the net effect after cAMP application on the reconstituted Kv11.1 channel was downregulation, but co-expression of ancillary subunits (KCNE1 or KCNE2) attenuated current inhibition.[12] I_{Kr} in guinea pig ventricular myocytes was suppressed[14] or increased[15] by isoproterenol. In our data, stimulation of $\beta_{1,2}$AR-coupled signaling (Figures 4 to 6) induced together cAMP and protein kinase A-dependent effects on I_{Kr} and Kv11.1 currents. The negative shift of I-V relation would oppose the inhibition of I_{Kr} by α_{1A}AR activation.

Arrhythmogenic significance

For the first time (to our knowledge), we showed adrenergic regulation of 2 LQT-associated Kv11.1 channels (N-terminal Y43D and pore K595E mutations), co-expressed with WT-Kv11.1 in a mammalian cell line. The currents had a loss-of-function phenotype but nevertheless maintained responses to phenylephrine and forskolin/IBMX similarly to the WT-Kv11.1 channel. With these mutant channels, acute sympathetic stimulation via α_{1A}AR would act to additionally increase APD and thus promote arrhythmogenesis. Evidence for possible contribution of α_{1A}AR-mediated triggers for loud noise-induced syncope is the fact that in the Kv11.1-Y43D proband, symptoms had been successfully eliminated by carvedilol, but in the case of Kv11.1-K595E, propranolol was ineffective.

Arrhythmogenic potential of α_{1A}AR-coupled mechanisms has the following support: phenylephrine-induced ventricular tachyarrhythmias in a canine LQT model in vivo[22]; the α_1-adrenoceptor agonist methoxamine facilitated the proarrhythmic effect of almokalant (a class III antiarrhythmic drug) in rabbit[23]; phenylephrine and methoxamine prolonged the APD of canine Purkinje fibers[4] and other animals[5]; and phenylephrine increased the transmural dispersion of ventricular depolarization (TDR) in LQT2 patients.[24] Although physiological regulation of ion channels through α_{1A}AR is not restricted only to I_{Kr}, our data

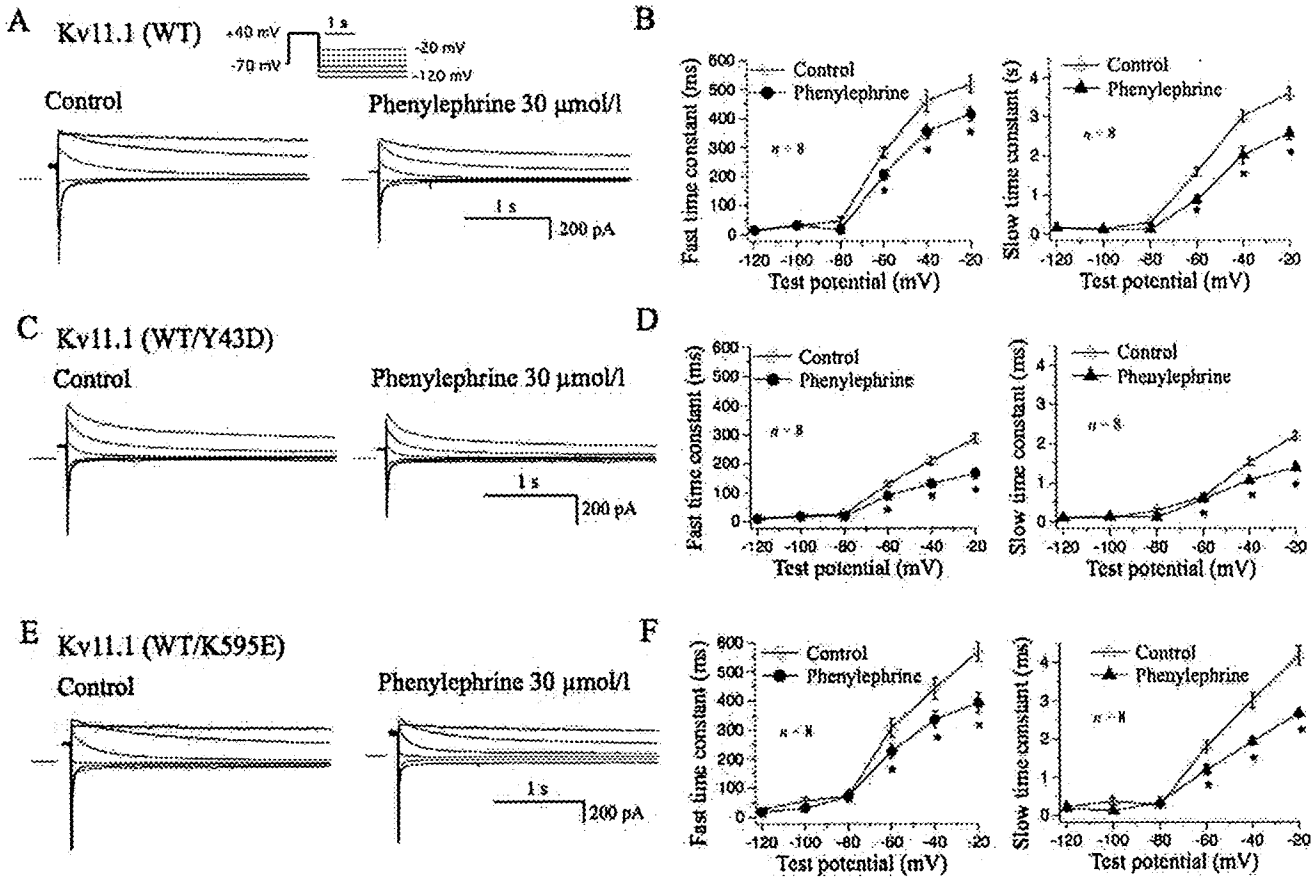

Figure 7 Deactivation kinetics of Kv11.1 currents. **A, C, E:** Representative Kv11.1 tail currents (WT, WT/Y43D, and WT/K595E, respectively) recorded at membrane potentials between −120 and −20 mV with a 20-mV increment after 2-second depolarizing step to +40 mV (**A, inset**) in control conditions and in the presence of 30 µmol/l phenylephrine. Similar to the results for I_{Kr} in HL-1 cardiomyocytes, deactivation of reconstituted WT and mutant Kv11.1 currents in CHO cells was facilitated by the α_{1A}AR agonist. **B, D, F:** The mean values of the fast and slow time constants of deactivation are plotted. The precise values of time constants at −60 mV are in Table 1 (see text).

suggest that it might be one of the currents involved in reported APD increase. In canine Purkinje fibers, the APD increase by phenylephrine was attributed mainly to I_K inhibition.[25]

Sympathetic stimulation is thought to initiate torsades de pointes in LQT by induction of triggered activity (early and delayed afterdepolarizations) and increase of TDR, which promotes propagation of premature electrical impulse.[26] In clinical studies, the effects of mainly $\beta_{1,2}$AR agonist epinephrine on QTc and duration of the interval between the peak and end of the T-wave on electrocardiogram ($T_{p\text{-}e}$, reflecting TDR) are known to be significantly longer in LQT1 than LQT2 at steady state.[28,29] On the other hand, in LQT2, an increase of QTc and $T_{p\text{-}e}$ by epinephrine is temporary and reversible at steady state (when comparisons with LQT1 in many studies were made[27,28]). Animal LQT models have shown the same dynamics in APD in the presence of epinephrine.[29] On the contrary, in LQT2 patients, phenylephrine was shown to prolong TDR considerably more than in LQT1.[24] Thus according to our results and the abovementioned reports, in LQT2 arrhythmia provoked shortly after sympathetic stress (loud noise), α_{1A}AR-mediated I_{Kr} reduction might be one potential triggering mechanism.

In brief, in the case of LQT2 and β-blockade, α_{1A}AR-mediated regulation of I_{Kr} could still cause sufficient derangements in ventricular repolarization to induce arrhythmia shortly after sympathetic stimulation. Higher resistance to β-blockers in LQT2 as well as the effectiveness of the α_1- and β-blocking agent labetalol[7] supports this statement. However, clinical investigations are needed to confirm this proposed mechanism.

Conclusion

This study investigated α_{1A}AR and $\beta_{1,2}$AR adrenergic regulation of 2 reconstituted Kv11.1 mutant channels found in loud noise-triggered symptomatic cases of congenital LQTS in comparison with wild-type Kv11.1 and native I_{Kr}. Although whole-cell currents from mutant Kv11.1 channels (co-expressed with wild-type Kv11.1) had a loss-of-function phenotype, they preserved negative regulation mediated through α_{1A}AR in a way similar to native I_{Kr} channel and wild-type Kv11.1.

The presented results implicate α_{1A}AR-coupled transduction in arrhythmogenesis in selected cases of congenital LQT2, specifically in patients with syncope after startled auditory stimuli, and suggest α_{1A}AR blockers as a beneficial treatment. It may worth clarifying α_{1A}AR regulation of long-QT-related Kv11.1 mutant channels, particularly in the cases of loud noise-induced arrhythmia or in patients resistant to β-blocking agents.

References

1. Moss AJ, Kass RS. Long QT syndrome: from channels to cardiac arrhythmias. J Clin Invest 2005;115:2018–2024.
2. Schwartz PJ, Priori SG, Spazzolini C, et al. Genotype–phenotype correlation in the long-QT syndrome: gene-specific triggers for life-threatening arrhythmias. Circulation 2001;103:89–95.
3. Wilde AAM, Jongbloed RJE, Doevendans PA, et al. Auditory stimuli as trigger for arrhythmic events differentiate HERG-related (LQTS2) patients from KVLQT1-related patients (LQTS1). J Am Coll Cardiol 1999;33:327–332.
4. Burashnikov A, Antzelevitch C. Differences in the electrophysiologic response of four canine ventricular cell types to α_1-adrenergic agonists. Cardiovasc Res 1999;43:901–908.
5. Drouin E, Charpentier F, Gauthier C. Alpha 1-adrenergic stimulation induces early afterdepolarizations in ferret Purkinje fibers. J Cardiovasc Pharmacol 1996;27:320–326.
6. Moss AJ, Zareba W, Hall J, et al. Effectiveness and limitations of β-blocker therapy in congenital long-QT syndrome. Circulation 2000;101:616–623.
7. Grubb BP. The use of oral labetalol in the treatment of arrhythmias associated with the long QT syndrome. Chest 1991;100:1724–1725.
8. Thomas D, Wu K, Wimmer A-B, et al. Activation of cardiac human ether-a-go-go related gene potassium currents is regulated by α_{1A}-adrenoceptors. J Mol Med 2004;82:826–837.
9. Jiang M, Dun W, Fan J-S, et al. Use-dependent 'agonist' effect of azimilide on the HERG channel. J Pharmacol Exp Ther 1999;291:1324–1336.
10. Bian J, Cui J, McDonald TV. HERG K+ channel activity is regulated by changes in phosphatidyl inositol 4,5-bisphosphate. Circ Res 2001;89:1168–1176.
11. Bian J-S, Kagan A, McDonald TV. Molecular analysis of PIP_2 regulation of HERG and I_{Kr}. Am J Physiol 2004;287:H2154–H2163.
12. Cui J, Melman Y, Palma E, et al. Cyclic AMP regulates the HERG K^+ channel by dual pathways. Curr Biol 2000;10:671–664.
13. Thomas D, Zhang W, Karle CA, et al. Deletion of protein kinase A phosphorylation sites in the HERG potassium channel inhibits activation shift by protein kinase A. J Biol Chem 1999;274:27457–27462.
14. Karle CA, Zitron E, Zhang W, et al. Rapid component I_{Kr} of the guinea-pig cardiac delayed rectifier K^+ current is inhibited by β_1-adrenoreceptor activation, via cAMP/protein kinase A-dependent pathways. Cardiovasc Res 2002;53:355–362.
15. Heath BM, Terrar A. Protein kinase C enhances the rapidly activating delayed rectifier potassium current, I_{Kr}, through a reduction in C-type inactivation in guinea-pig ventricular myocytes. J Physiol 2000;522.3:391–402.
16. Claycomb WC, Lanson NA, Stallworth BS, et al. HL-1 cells: a cardiac muscle cell line that contracts and retains phenotypic characteristics of the adult cardiomyocytes. Proc Natl Acad Sci U S A 1998;95:2979–2984.
17. Yang Z, Shen W, Rottman JN, et al. Rapid stimulation causes electrical remodeling in cultured atrial myocytes. J Mol Cell Cardiol 2005;38:299–308.
18. Tutor AS, Delpón E, Caballero R, et al. Association of 14-3-3 proteins to β_1-adrenergic receptors modulates Kv11.1 K^+ channel activity in recombinant systems. Mol Biol Cell 2006;17:4666–4674.
19. Hamill OP, Marty A, Neher E, et al. Improved patch-clamp techniques for high-resolution current recordings from cells and cell-free membrane patches. Pflügers Arch 1981;391:85–100.
20. Sanguinetti MC, Jiang C, Curran ME, et al. A mechanistic link between an inherited and an acquired cardiac arrhythmia: HERG encodes the I_{Kr} potassium channel. Cell 1995;81:299–307.
21. Balla T, Várnai P. Visualizing cellular phosphoinositide pools with GFP-fused protein-modules. Sci STKE 2002;125:PL3.
22. Ben-David J, Zipes DP. α-Adrenoceptor stimulation and blockade modulates cesium-induced early afterdepolarizations and ventricular tachyarrhythmias in dogs. Circulation 1990;82:225–233.
23. Carlsson L, Abrahamsson C, Andersson B, et al. Proarrhythmic effects of the class III agent almokalant: importance of infusion rate, QT dispersion, and early afterdepolarizations. Cardiovasc Res 1993;27:2186–2193.
24. Khositseth A, Nemec J, Hejlik J, et al. Effect of phenylephrine provocation on dispersion of repolarization in congenital long QT syndrome. Ann Noninvasive Electrocardiol 2003;8:208–214.
25. Lee JH, Rosen MR. Alpha 1-adrenergic receptor modulation of repolarization in canine Purkinje fibers. J Cardiovasc Electrophysiol 1994;5:232–240.
26. Antzelevitch C, Shimizu W. Cellular mechanisms underlying the long QT syndrome. Curr Opin Cardiol 2002;17:43–51.
27. Noda T, Takaki H, Kurita T, et al. Gene-specific response of dynamic ventricular repolarization to sympathetic stimulation in LQT1, LQT2, and LQT3 forms of congenital long QT syndrome. Eur Heart J 2002;23:975–983.
28. Shimizu W, Noda T, Takaki H, et al. Diagnostic value of epinephrine test for genotyping LQT1, LQT2, and LQT3 forms of congenital long QT syndrome. Heart Rhythm 2004;3:276–283.
29. Shimizu W, Antzelevitch C. Differential effects of beta-adrenergic agonists and antagonists in LQT1, LQT2 and LQT3 models of the long QT syndrome. J Am Coll Cardiol 2000;35:778–786.

KCNE2 modulation of Kv4.3 current and its potential role in fatal rhythm disorders

Jie Wu, PhD,* Wataru Shimizu, MD, PhD,† Wei-Guang Ding, MD, PhD,‡ Seiko Ohno, MD, PhD,§ Futoshi Toyoda, PhD,‡ Hideki Itoh, MD, PhD,¶ Wei-Jin Zang, MD, PhD,* Yoshihiro Miyamoto, MD, PhD,‖ Shiro Kamakura, MD, PhD,† Hiroshi Matsuura, MD, PhD,‡ Koonlawee Nademanee, MD, FACC,# Josep Brugada, MD,** Pedro Brugada, MD,†† Ramon Brugada, MD, PhD, FACC,‡‡ Matteo Vatta, PhD,§§¶¶ Jeffrey A. Towbin, MD, FAAP, FACC,§§ Charles Antzelevitch, PhD, FACC, FAHA, FHRS,‖‖ Minoru Horie, MD, PhD¶

*From the *Pharmacology Department, Medical School of Xi'an Jiaotong University. Xi'an, Shaanxi, China, †Division of Cardiology, Department of Internal Medicine, National Cardiovascular Center, Suita, Japan, ‡Department of Physiology, Shiga University of Medical Science, Ohtsu, Japan, §Department of Cardiovascular Medicine, Kyoto University of Graduate School of Medicine, Kyoto, Japan, ¶Department of Cardiovascular Medicine, Shiga University of Medical Science, Shiga, Japan, ‖Laboratory of Molecular Genetics, National Cardiovascular Center, Suita, Japan, #Department of Medicine (Cardiology), University of Southern California, Los Angeles, California, **Cardiovascular Institute, Hospital Clinic, University of Barcelona, Barcelona, Spain, ††Heart Rhythm Management Centre, Free University of Brussels (UZ Brussel) VUB, Brussels, Belgium, ‡‡School of Medicine, Cardiovascular Genetics Center, University of Girona, Girona, Spain, §§Departments of Pediatrics, Baylor College of Medicine, Houston, Texas, ¶¶Department of Molecular Physiology and Biophysics, Baylor College of Medicine, Houston, Texas, and ‖‖Masonic Medical Research Laboratory, Utica, New York.*

BACKGROUND The transient outward current I_{to} is of critical importance in regulating myocardial electrical properties during the very early phase of the action potential. The auxiliary β subunit *KCNE2* recently was shown to modulate I_{to}.

OBJECTIVE The purpose of this study was to examine the contributions of *KCNE2* and its two published variants (M54T, I57T) to I_{to}.

METHODS The functional interaction between Kv4.3 (α subunit of human I_{to}) and wild-type (WT), M54T, and I57T *KCNE2*, expressed in a heterologous cell line, was studied using patch-clamp techniques.

RESULTS Compared to expression of Kv4.3 alone, co-expression of WT *KCNE2* significantly reduced peak current density, slowed the rate of inactivation, and caused a positive shift of voltage dependence of steady-state inactivation curve. These modifications rendered Kv4.3 channels more similar to native cardiac I_{to}. Both M54T and I57T variants significantly increased I_{to} current density and slowed the inactivation rate compared with WT *KCNE2*. Moreover, both variants accelerated the recovery from inactivation.

CONCLUSION The study results suggest that *KCNE2* plays a critical role in the normal function of the native I_{to} channel complex in human heart and that M54T and I57T variants lead to a gain of function of I_{to}, which may contribute to generating potential arrhythmogeneity and pathogenesis for inherited fatal rhythm disorders.

KEYWORDS Cardiac arrhythmia; M54T variation; I57T variation; *KCNE2*; Kv4.3; Sudden cardiac death

ABBREVIATIONS **CHO** = Chinese hamster ovary; **HERG** = human ether-a-go-go related gene; **WT** = wild type

(Heart Rhythm 2010;7:199–205)

Introduction

Classic voltage-gated K^+ channels consist of four pore-forming (α) subunits that contain the voltage sensor and ion selectivity filter[1,2] and accessory regulating (β) subunits.[3] *KCNE* family genes encode several kinds of β subunits consisting of single transmembrane-domain peptides that co-assemble with α subunits to modulate ion selectivity, gating kinetics, second messenger regulation, and the pharmacology of K^+ channels. Association of the *KCNE1* product minK with the α subunit Kv7.1 encoding *KCNQ1* forms the slowly activating delayed rectifier K^+ current I_{Ks} in the heart.[4,5] In contrast, association of the *KCNE2* product MiRP1 with the human ether-a-go-go related gene (HERG) forms the cardiac rapid delayed rectifier K^+ current I_{Kr}.[6]

The first two authors contributed equally to the original concept and the authorship of this study. This study was supported by grants from the Ministry of Education, Culture, Sports, Science, Technology Leading Project for Biosimulation to Dr. Horie; Health Sciences Research grants (H18-Research on Human Genome-002) from the Ministry of Health, Labour and Welfare, Japan to Drs. Shimizu and Horie; the National Natural Science Foundation of China (Key Program, No.30930105; General Program, No. 30873058, 30770785) and the National Basic Research Program of China (973 Program, No. 2007CB512005) and CMB Distinguished Professorships Award (No. F510000/G16916404) to Dr. Zang; and National Institutes of Health Grant HL47678 and Free and Accepted Masons of New York State and Florida to Dr. Antzelevitch. **Address reprint requests and correspondence:** Dr. Minoru Horie, Department of Cardiovascular and Respiratory Medicine, Shiga University of Medical Science, Otsu, Shiga 520-2192, Japan. E-mail address: horie@belle.shiga-med.ac.jp. (Received August 20, 2009; accepted October 7, 2009.)

1547-5271/$ -see front matter doi:10.1016/j.hrthm.2009.10.012